Computational and Structural Biotechnology Journal 19 (2021) 384–400

COMPUTATIONAL AND STRUCTURAL BIOTECHNOLOGY JOURNAL

journal homepage: www.elsevier.com/locate/csbj

Microbial risk assessment of *Nocardia cyriacigeorgica* in polluted environments, case of urban rainfall water

Florian Vautrin [a,e], Petar Pujic [f,1], Christian Paquet [b], Emmanuelle Bergeron [a], Delphine Mouniée [a], Thierry Marchal [c], Hélène Salord [d], Jeanne-Marie Bonnet [b], Benoit Cournoyer [a], Thierry Winiarski [e], Vanessa Louzier [b,1,*], Veronica Rodriguez-Nava [a,d,1,*]

[a] *UMR Ecologie Microbienne, CNRS 5557, INRA 1418, Research Team on Bacterial Opportunistic Pathogens and Environment, VetAgro Sup and University, Lyon 1, F-69363 Lyon, France*
[b] *APCSe, Agressions Pulmonaires et Cardiovasculaires dans le Sepsis, VetAgro Sup – Campus vétérinaire de Lyon, 69280 Marcy l'Etoile, France*
[c] *Laboratoire vétérinaire d'histopathologie, VetAgro Sup – Campus vétérinaire de Lyon, 69280 Marcy l'Etoile, France*
[d] *Observatoire Français des Nocardioses, Institut des Agents Infectieux (IAI), Centre de Biologie et Pathologie Nord, Hôpital de la Croix-Rousse, 69317 Lyon, France*
[e] *UMR LEHNA, CNRS 5023, ENTPE, University Lyon 1, F-69622 Villeurbanne, France*
[f] *UMR Ecologie Microbienne, CNRS 5557, INRA 1418, VetAgro Sup and University, Lyon 1, F-69622, Villeurbanne, France*

ARTICLE INFO

Article history:
Received 15 September 2020
Received in revised form 12 December 2020
Accepted 13 December 2020
Available online 29 December 2020

Keywords:
Nocardia
Opportunistic pathogen
Environment
Murine model of transient immunoparalysis
Urban pollution
Hsp65 metabarcoding

ABSTRACT

Urban Infiltration Basins (UIBs) are used to manage urban runoff transfers and feed aquifers. These UIBs can accumulate urban pollutants and favor the growth of potentially pathogenic biological agents as *Nocardia*.

Objectives: To assess the spatio-temporal dynamics of pathogenic *Nocardia* in UIBs and to stablish phylogenetic relationships between clinical and UIB *N. cyriacigeorgica* strains. To assess pathogenicity associated with environmental *N. cyriacigeorgica* using an animal model, and to identify genetic elements that may be associated to its virulence.

Methods: A well-characterized UIB in terms of chemical pollutants from Lyon area was used in this study during a whole year. Cultural and Next-Generation-Sequencing methods were used for *Nocardia* detection and typing. Clinical and environmental isolates phylogenetic relationships and virulences were compared with Multilocus-Sequence-Analysis study together with a murine model.

Results: In autumn, *N. cyriacigeorgica* and *N. nova* were the pathogenic most prevalent species in the UIB. The complex *N. abscessus/asiatica* was also detected together with some other non-pathogenic species. The presence of pathogenic *Nocardia* was positively correlated to metallic trace elements. Up to 1.0×10^3 CFU/g sediment of *N. cyriacigeorgica* and 6 OTUs splited in two different phylogroups were retrieved and were close to clinical strains. The EML446 tested UIB isolate showed significant infectivity in mice with pulmonary damages similar to clinical clone (GUH-2).

Conclusion: Hsp65 marker-based metabarcoding approach allowed detecting *N. cyriacigeogica* as the most abundant *Nocardia* pathogenic species in a UIB. Metal trace elements-polluted environments can be reservoirs of pathogenic *Nocardia* which may have a similar virulence to clinical strains.

1. Introduction

Nocardia are Gram-positive facultative intracellular bacteria responsible for nocardiosis. Manifestations of disease range from cutaneous infection caused by traumatic inoculation of the organism in a normal host to severe pulmonary or central nervous system (CNS) disease in an immunocompromised host [1]. Pulmonary infection is the most frequent clinical form which is similar to pneumonia in 80% of cases and that can be fatal in patients who are immunocompromised or affected by chronic pulmonary diseases [2,3]. *Nocardia* cells are ubiquitous in the environ-

* Corresponding authors at: UMR Ecologie Microbienne, CNRS 5557, INRA 1418, 8 avenue Rockefeller, 69373 Lyon cedex, France.

E-mail addresses: florianvautrin@gmail.com (F. Vautrin), petar.pujic@univ-lyon1.fr (P. Pujic), christian.paquet@vetagro-sup.fr (C. Paquet), emmanuelle.bergeron@univ-lyon1.fr (E. Bergeron), delphine.mouniee@univ-lyon1.fr (D. Mouniée), thierry.marchal@vetagro-sup.fr (T. Marchal), helene.salord@chu-lyon.fr (H. Salord), jeanne-marie.bonnet@vetagro-sup.fr (J.-M. Bonnet), benoit.cournoyer@vetagro-sup.fr (B. Cournoyer), thierry.winiarski@entpe.fr (T. Winiarski), vanessa.louzier@vetagro-sup.fr (V. Louzier), veronica.rodriguez-nava@univ-lyon1.fr (V. Rodriguez-Nava).

[1] These authors contributed equally to this work.

https://doi.org/10.1016/j.csbj.2020.12.017

ment but distribution biases per species are still poorly documented. Nocardiosis are caused by inhalation of these bacteria from aerosolized soils. *Nocardia* cells are metabolically versatile, and some species such as *N. cyriacigeorgica* can harbor genes involved in the degradation of petrol-derivatives [4–6]. This property likely explains the tropism of *Nocardia* cells for polluted environments [7]. *N. cyriacigeorgica* is also known for its ability to propagate in alveolar macrophages, inducing pulmonary damage. Some more virulent strains are able to disseminate and reach the brain [8]. Prevalence of *N. cyriacigeorgica* in nocardiosis was estimated to be around 20% in the USA [9], 25% in Spain [10] and 13% in France with a global nocardiosis incidence between 0.33 and 0.87/100 000 inhabitants [11]. The environmental occurrence, persistence and enrichment of *N. cyriacigeorgica* remain to be defined. Here, the hypothesis of a tropism of *Nocardia* cells, and *N. cyriacigeorgica*, for biotopes found in a city, was tested because of their ability at using petrol-derivatives as carbon sources. Furthermore, we have tested the hypothesis of an on-going evolution in the virulence traits of these urban *Nocardia* cells. The hypothesis was that city strains should have a reduced but significant virulence in comparison with clinical isolates, when tested on mice as an alternative host system.

Nocardia cells together with other microorganisms such as *Pseudomonas aeruginosa*, *Aeromonas caviae* and fecal indicators, have recently been shown to be recurrent contaminants of the urban deposits of a detention basin of a Stormwater Infiltration System (SIS) located in the Lyon area (France). Presence of *Nocardia* cells at the outflow of this basin redirecting to an Urban Infiltration Basin (UIB) were also observed, but the transferred species from the detention to the UIB remained to be defined [12]. To decrease the environmental impacts of runoff flooding, SISs have been constructed all over the world to manage runoff transfers and favor the recharging of local aquifers. Today, >5000 SISs are monitored around the world [13]. Runoff waters getting into SISs are loaded with organic and mineral particles such as PAHs (Polycyclic Aromatic Hydrocarbons), PCBs (Polychlorinated Biphenyls), heavy metals and microorganisms [14], which accumulate on the surface of the infiltration basins to generate the so-called "urban sediments" [15].

The presence of pathogenic microorganisms in these sediments constitutes a public health risk because they can contribute in multiple ways at disseminating hazardous biological agents either through (i) a transfer into natural water systems such as an aquifer which can be used for gardening [16], (ii) a contamination of animals feeding in these systems that can come into contact with humans (dogs, cats, rats, birds), or (iii) through an aerosolization towards environments with environmental characteristics (moisture, pollutants, etc.) that may also favor their growth (moist urban zones, gas-stations, major road axes, petrochemical factories, etc.) and the consequent inhalation of these microbial cells by the local populations. It has to be noted that aerosolized bacterial cells can migrate over large distances as observed for *P. aeruginosa*, *Escherichia coli*, and *Klebsiella pneumoniae* [17].

Moreover, the interest of studying UIBs is that, due to their heterogeneity (gradient of pollutants and moisture), they can mimic various environments that can be found in many other different locations, such as urban water areas (blue-zones), green areas or puddles after a rainfall event.

The aims of this study were thus to determine the spatiotemporal distribution biases of *Nocardia* cells and pathogenic species such as *N. cyriacigeorgica* in an urban SIS, and to evaluate their hazards for local populations. Epidemiological molecular investigations were performed to define the phylogenetic relations between SIS *N. cyriacigeorgica* isolates and clinical strains. The virulence of these isolates was then compared using a double-hit murine model of transient immunoparalysis, but also through an analysis of virulence gene content or virulome.

2. Materials and methods

2.1. Stormwater infiltration system

The studied SIS (named Django-Reinhardt) is part of a long term monitoring site of OTHU (Field Observatory for Urban Water Management; http://www.graie.org/othu/) [18]. It is located in Chassieu, France (eastern part of Lyon). This system has been operational for approximately 40 years and consists of a detention basin receiving runoff water from the stormwater network, and discharging its waters into an Urban Infiltration Basin (UIB), hereafter named DRIB (Django-Reinhardt Infiltration Basin) (Fig. 1). The DRIB has a 1 ha surface and a volume of 61,000 m^3. The drained surfaces are in a stabilized industrial area, and the main pollutants found in the accumulated sediments are heavy metals, cyanides, inks, fats, hydrocarbons and solvents [19].

The DRIB has been extensively studied. Some of its sediments properties were characterized according to normalized procedures such as ISO10390 for pH and ISO13320 for granulometry. Soil moisture was determined by comparative weighing before and after 24 h at 105 °C. Additional DRIB data were also extracted from the Gessol report, and indicated a mean of 2–3.5 mg for the sum of the 16 well-defined PAHs /kg dry sediment [19]. These values were found equivalent to those of industrial soils, *e.g.* 3.5 mg/kg according to Muntean et al., while PAHs levels in unpolluted soils were 4–12 μg/kg [20,21].

2.2. Sampling

Urban sediments of the DRIB were sampled during three different sampling campaigns, one per season (autumn (November), spring (April) and summer (July) 2015–2016) in three contrasted areas: near the detention basin discharging pipe (inflow zone), in the middle of the basin (bottom zone), and at the southern end of the basin (upper zone, five samples per area). These positions match different concentrations of pollutants, distinct hydrological behaviors, soil moisture and vegetation (Fig. 1).

2.3. Physical-chemical parameters statistical analyses

All datasets were analyzed with the R software (V.3.1.3) [27]. The distribution of the physical–chemical parameters (PAHs, trace metal elements (Cd, Cu, Hg, Pb and Zn), granulometry, water content) and relative abundance of *Nocardia* (pathogenic *vs* non-pathogenic) was represented by a between-class analysis (BCA) allowing a longitudinal analysis. Packages ade4 [28], mixOmics and RVAideMemoire [29] were used. Trace elements and metals were log transformed because they are not normally distributed. All the other parameters were normally distributed according to a Shapiro test. The diversity within each individual sample was estimated using the non-parametric Shannon index. Statistical analyses were performed using ANOVA2 and normality of the residues was tested in order to establish the significance of the groupings. Only p-values lower to 0.05 were considered as statistically significant. The correlogram and p-values were obtained on R software using the ade4, corrplot and Hmisc packages [30].

2.4. Identification approaches

2.4.1. Culture-independent approach

A metabarcoding approach by using *hsp65* gene was used. Genomic DNA from environmental samples of the DRIB was

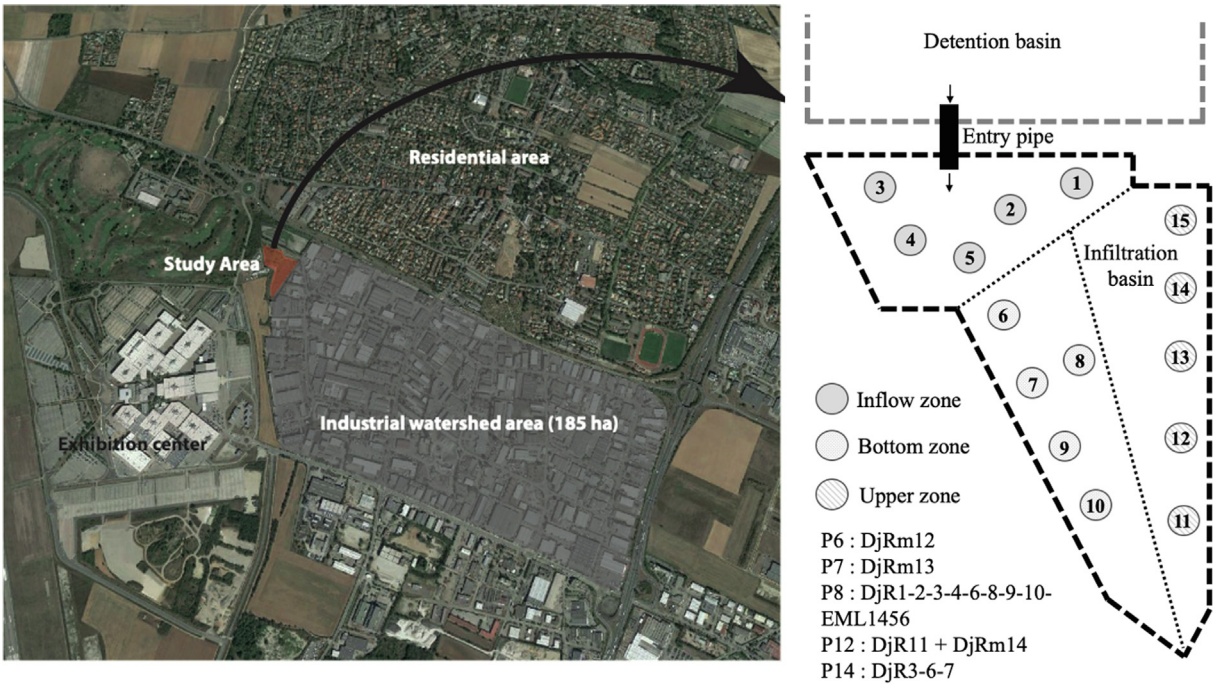

Fig. 1. Aerial image of the Django-Reinhardt infiltration basin (DRIB) and position of the sampling points in the DRIB and placement of the three different sampling areas (inflow zone, bottom zone and upper zone). Px: DRIB sample point in which *N. cyriacigeorgica* was isolated and respective reference code.

extracted using the FastDNA SPIN Kit for Soil (MP Biomedicals, France) according to the manufacturer's instructions. Amplifications were performed on the *hsp65* gene (Table 1) using PuRe-Taq™ Ready-To-Go PCR Beads (GE Healthcare) in a final volume of 50 µL and sequenced (together with purification and quality control) by Biofidal (https://www.biofidal.com/) using high-throughput Illumina MiSeq with 2 × 250 bp, paired-end chemistry to obtain 20,000 paired reads per sample. Bioinformatics analysis were performed using the MOTHUR pipeline [31], and according to the protocol previously defined by Marti et al. [16]. The number of sequences was normalized between the samples and was set to 7,128 sequences. *Hsp*65-OTUs at a 99% cutoff for species level identification were used.

2.4.2. Culture-dependent approach

Diluted suspensions of the urban sediments from the DRIB were cultured on Bennett and Middlebrook 7H10 agar (Thermo Fisher ®) semi-selective medium, and colonies with morphological features typical of *Nocardia* (presenting a white and powdery aspect and embedded in the agar) were purified, and then identified at the species level by sequencing and analysis of the 16S rRNA gene, according to Rodriguez-Nava et al. [22] and following the CLSI guidelines of similarity percentages greater than or equal to 99.6% [27]. When facing ambiguity or when identification is not possible with this gene we decided to use a more discriminative one according to Sanchez-Herrera et al. [24].

N. cyriacigeorgica isolates were obtained from the 2015–2016 sampling campaign. An additional *N. cyriacigeorgica* isolate

Table 1
PCR primers and DNA amplification conditions for *rrs, hsp65, sodA, secA1* genes and *Nocardia* specific PCR.

Target	Length (bp)	Forward primer (5′–3′)		Reverse primer (5′–3′)		PCR cycling conditions	Reference
		Primer name	Sequence	Primer name	Sequence		
rrs	569	Noc1	GCTTAACACATGCAAGTCG	Noc2	GAATTCCAGTCTCCCCTG	5 min 94 °C; 40× 1 min 94 °C, 1 min 58 °C, 1 min 72 °C; 10 min 72 °C	Rodriguez-Nava et al. 2006 [22]
hsp65	401	TB11	ACCAACGATGGTGTGTCCAT	TB12	CTTGTCGAACCGCATACCCT	5 min 94 °C; 35x 1 min 94 °C, 1 min 55 °C, 1 min 72 °C; 10 min 72 °C	Telenti et al. 1993 [23]
sodA	406	SodV1	CACCAYWSCAAGCACCA	SodV2	CCTTGACGTTCTGGTACTG	5 min 94 °C; 35× 1 min 94 °C, 1 min 52 °C, 1 min 72 °C; 10 min 72 °C	Sánchez-Herrera et al. 2017 [24]
secA1	469	SecA1	GTAAAACGACGGCCAGG ACAGYGAGTGGATGGGYCGSGTGCACCG	SecA2	CAGGAAACAGCTATGACGCGGACG ATGTAGTCCTTGTC	5 min 95 °C; 35× 1 min 95 °C, 1 min 60 °C, 1 min 72 °C; 10 min 72 °C	Conville et al. 2006 [25]
NG*	590	NG1	ACCGACAAGGGGG	NG2	GGTTGTAAACCTCTTTCGA	11 min 94 °C; 30× 1 min 94 °C, 20 sec 55 °C, 1 min 72 °C; 10 min 72 °C	Laurent et al. 1999 [26]

Note: Y = C or T, W = A or T and S = C or G, * NG = *Nocardia* Genus.

Table 2
List of SIS and clinical strains used in this study, and their origin, main features and MLSA-phylogroups.

Patient record	Sample date	Sample	Host Immunosuppressed	Tropism of nocardiosis or origin of isolate	Location	MLSA-phylogroup
OFN.4	03/2015	Pus from cutaneous abscess	Yes	Cutaneous	Neuilly sur Seine	PI
OFN.5	10/2017	Bronchial aspirate	Yes	Lung	Lyon	PI
OFN.6	06/2010	Pus from cerebral abscess	Yes	Brain	Bron	PI
OFN.7	06/2015	Bronchial aspirate	No	Brain[d]	Bron	PI
OFN.13	02/2015	Pus from skin abscess	Yes	Lung[d]	Montpellier	PI
OFN.14	03/2015	Cervical biopsy	Yes	Brain	Montpellier	PI
DjRm.12	11/2015	UIB *hsp65* metabarcoding	–	Bottom	Chassieu	PI
DjRm.14	11/2015	UIB *hsp65* metabarcoding	–	Upper	Chassieu	PI
OFN.8	02/2016	Cervical biopsy	NA	Brain	Metz	PII
OFN.9	11/2015	Bronchial aspirate	Yes	Lung	Montpellier	PII
OFN.10	11/2015	Bronchial aspirate	Yes	Lung	Aulney sous Bois	PII
OFN.11	07/2011	Pus from cutaneous abscess	No	Cutaneous	Belley	PII
OFN.12	04/2014	Blood culture	Yes	Brain[d]	Réunion island	PII
OFN.1	02/2013	Blood culture	No	Lung[d]	La Roche sur Yon	PIII
OFN.2	03/2016	Pleural puncture	Yes	Lung	Agen	PIII
OFN.3	01/2016	Lung biopsy	Yes	Lung	Tours	PIII
EML446	04/2013	UIB polluted sediments	–	Bottom	Chassieu	PIII
EML1456	11/2015	UIB polluted sediments	–	Bottom	Chassieu	PIII
DjR.1	11/2015	UIB polluted sediments	–	Bottom	Chassieu	PIII
DjR.2	11/2015	UIB polluted sediments	–	Bottom	Chassieu	PIII
DjR.3	07/2016	UIB polluted sediments	–	Upper	Chassieu	PIII
DjR.4	11/2015	UIB polluted sediments	–	Bottom	Chassieu	PIII
DjR.5	07/2016	UIB polluted sediments	–	Upper	Chassieu	PIII
DjR.6	11/2015	UIB polluted sediments	–	Bottom	Chassieu	PIII
DjR.7	07/2016	UIB polluted sediments	–	Upper	Chassieu	PIII
DjR.8	07/2016	UIB polluted sediments	–	Bottom	Chassieu	PIII
DjR.9	07/2016	UIB polluted sediments	–	Bottom	Chassieu	PIII
DjR.10	07/2016	UIB polluted sediments	–	Bottom	Chassieu	PIII
DjR.11	04/2016	UIB polluted sediments	–	Upper	Chassieu	PIII
DjRm.13	07.2016	UIB *hsp65* metabarcoding	–	Bottom	Chassieu	PIII

Note: [d] indicates a disseminated case of nocardiosis, NA: data not available, MLSA: multilocus sequence analysis, SIS: stormwater infiltration system

(EML446), obtained from a bottom area sediment sample in a previous campaign in 2013, was added to our work. It is the first strain of the pathogenic *N. cyriacigeorgica* species that has been isolated in an anthropized environment in Europe. Sampling conditions for this last isolate were identical, just the culture media changed as the Actinomytes isolation Agar (DifcoTM) culture media was used in that case. The list of isolates is presented in Table 2.

2.5. Phylogenetic analysis

DNA sequences (*rrs-hsp65-sodA-secA1*) were generated for the DRIB *N. cyriacigeorgica* isolates (n = 13). These sequences were compared with those of clinical *N. cyriacigeorgica* (n = 14), and of other *Nocardia* reference strains (n = 10). The following strains were considered: *N. abscessus* DSM 44432 ^{T}, *N. anaemiae* DSM 44821 ^{T}, *N. asteroides* ATCC 19247 ^{T}, *N. brasiliensis* ATCC 19296 ^{T}, *N. cyriacigeorgica* DSM 44484 ^{T}, *N. farcinica* IFM 10152 ^{T}, *N. nova* DSM 44481 ^{T}, *N. otitidiscaviarum* ATCC 14629 ^{T}, *N. vinacea* JCM 10988 ^{T} and *N. cyriacigeorgica* GUH-2, the reference pathogenic strain isolated from a fatal case of nocardiosis after a renal transplant in the 1970s [32]. These reference strains chosen in this study are phylogenetically closely related to *N. cyriacigeorgica* according to Yassin et al. [33]. Clinical *N. cyriacigeorgica* were obtained from OFN (French Observatory of Nocardiosis, http://ofn.univ-lyon1.fr/), and originated from French patients affected by nocardiosis (cutaneous, pulmonary, and cerebral infections) (Table 2). By selecting these strains, we obtained a good representation of the main clinical forms of this disease that encompassed the environmental sampling period of this study (2015–2016).

Bacterial DNAs of these strains were extracted by the boiling method using achromopeptidase (10 $U.\mu L^{-1}$, Sigma-Aldrich). Amplifications of the following genes were performed: 16S rRNA *(rrs)* (positions 64 to 663, *N. cyriacigeorgica* DSM 44484 ^{T}), *hsp65* (positions 398 to 836, *N. cyriacigeorgica* DSM 44484 ^{T}), *sod*A (positions 99 to 505, *N. cyriacigeorgica* DSM 44484 ^{T}), *secA1* (positions 396 to 864, *N. cyriacigeorgica* DSM 44484 ^{T}). PCR were performed using PuReTaq™ Ready-To-Go PCR Beads (GE Healthcare) in a final volume of 25 µL with 200 ng of DNA. Primers and PCR conditions are listed in Table 1. PCR products were sequenced by Biofidal (Vaulx-en-Velin, France). Multiple alignments were generated by ClustalW using Seaview version 4.4.2 [34]. Only for the phylogenetic analysis of *N. cyriacigeorgica* species based on *hsp65*-gene, we added to our sequences dataset i) some sequences from the historically known *hsp65*-based genotypes [9,35–37] that are available on Genbank, and ii) some sequences coming from our metabarcoding analysis of strains isolated from the DRIB. For MLSA (Multilocus Sequence Analysis), the *rrs-hsp65-sodA-secA1* sequences were concatenated (1,845 bp). Phylogenetic relationships were resolved using the maximum-likelihood method through the MEGA software, version 7.0.16 [38]. A cutoff of 99.5% was used for MLSA-phylogroups differentiation. Bootstrapping using 1,000 replicates was performed for each analysis (single locus or multiple ones).

2.6. Comparative analysis of virulence genes among a SIS *N. cyriacigeorgica* isolate

The EML446 strain was selected to represent the SIS *N. cyriacigeorgica* isolates. This strain was chosen as it has been extensively

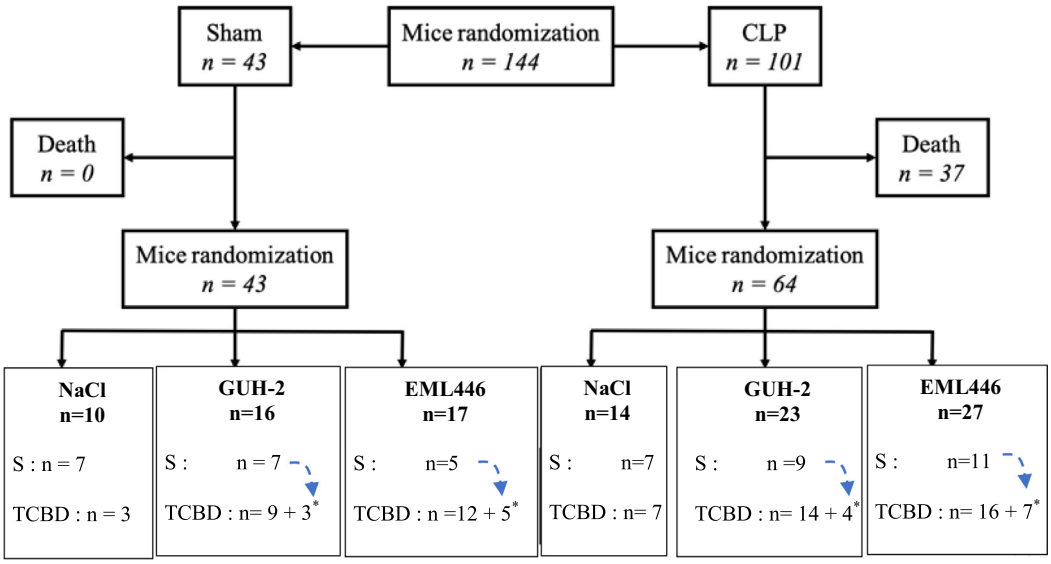

Fig. 2A. Study design describing the experiment made with the immunosuppressed CLP (cecal ligature and puncture) (30%) murine model to compare the virulence of the SIS (stormwater infiltration system) and clinical *N. cyriacigeorgica* representative strains. Sham = mice that underwent laparotomy with exposition of the cecum but without CLP. CLP = intestinal tract externalization and puncture performed as described by Restagno et al. [43]. S = Survival experiment. TCBD = Time Course Bacterial Detection experiment. n = number of individuals in each group. * = surviving mice at the end of the 'S' experiment retrieved for 'TCBD' one at D33 (GUH-2) or D41 (EML446).

Group	Day	Mice number for TCBD
Sham GUH-2	4	5
	10	3
	33	1 + 3*
Sham EML446	4	5
	10	5
	33	2
	41	5 *, a)
CLP GUH-2	4	5
	10	5
	33	4 + 4*
CLP EML446	4	7 b)
	10	4
	33	5
	41	7 *, c)

Fig. 2B. Mice distribution for the Time Course Bacterial Detection experiment (TCBD). * = Surviving mice from the end of the Survival experiment retrieved at the end of the TCBD one. a) lungs of two mice will be reserved for histological analysis, b) lungs of one mouse will be reserved for histological analysis. c) lungs of three mice and brains of two mice will be reserved for histological analysis.

studied in our laboratory. It was grown on BHI agar medium (Difco BD), and its genomic DNA was extracted with the standard phenol–chloroform-isoamyl alcohol method [39]. Genome sequencing was performed on a HiSeq2000 Illumina system by GATC (Mulhouse, France). Assemblage and annotation were performed on MicroScope [40]. Contigs are available from the BioProject PRJNA542857 [41]. Comparative analyses were performed against *N. farcinica* IFM 10152 ^{T}, *Mycobacterium tuberculosis* H37Rv (both already available on NCBI) and the GUH-2 genome reported by Zoropogui et al. [42]. This strain has been chosen as representative of clinical strains because it has been commonly used as model strain in many pathophysiology studies [8]. Virulence genes targeted were those identified by Zoropogui et al. in the genomic study of GUH-2 strain [42].

2.7. Virulence tests with a double-hit murine model of transient immunoparalysis

2.7.1. General issues

All experiments presented below were approved by the Institutional Animal Care and Use Committee at VetAgro Sup (proposal 1403) in accordance with the European Convention for the Protection of Vertebrate Animals used for Experimental and other Scientific Purposes.

Male mice C57BL/6J (Charles River, L'Arbresle, France) of 7–9 weeks of age (20–25 g) were housed for one week before beginning the experiments at the Veterinary school (VetAgro Sup, Marcy l'Etoile, France). A 12 h' dark/light cycle was applied over all experiments. Immunoparalysis of some mice was induced via a moderate cecal ligation and puncture (CLP 30%), and *Nocardia* cells (the SIS EML446 or GUH-2 clinical isolate) were then instilled in the pulmonary airways to test their virulence properties. The CLP procedure (externalization, puncture, antibiotic treatment and pain control) was performed as described in Restagno et al. [43]. Sham (control-operated mice) underwent laparotomy with exposition of the cecum but without CLP.

The starting mouse population was made of 144 individuals. Animals were randomly split into six groups: 1) Sham-NaCl mice which received a saline solution; 2) Sham-GUH-2 mice instilled with GUH-2; 3) Sham-EML446 mice instilled with EML446; 4) CLP-NaCl mice which received a saline solution; 5) CLP-GUH-2 mice instilled with GUH-2; and 6) CLP-EML446 mice instilled with EML446. Due to the unpredictable exact mortality rate induced by

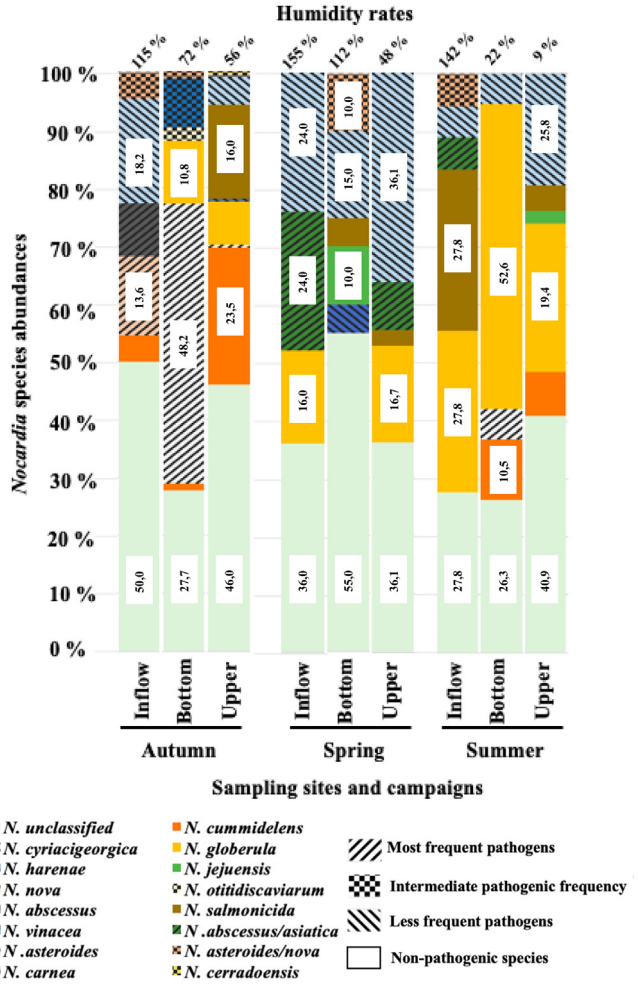

Fig. 3. DNA metabarcoding analysis of *Nocardia* genetic diversity among SIS (stormwater infiltration system) sediment samples using the *hsp65* target. A total of 7,128 sequences per sample was analyzed. The relative proportion of the detected *Nocardia* species is presented in %. Species representing>1% over the total number of reads are indicated and only values > 10% are indicated. The classification of most/intermediate/less frequent pathogens was based on the most clinically relevant species in France epidemiology according to Lebeaux et al. [11].

CLP, more mice were CLP-treated than Sham-treated to reach the right number of CLP subjects. The aim of the "*Nocardia*-free" groups (*i.e.,* Sham-NaCl and CLP-NaCl) was to ensure that mortality was not CLP-dependent. The final experimental design is shown in Figs. 2A and 2B.

Prior studies were performed with three different bacterial concentrations (data not shown) to determine the sublethal dose. Strains GUH-2 and EML446 were cultivated in BHI medium and adjusted to 2.0×10^7 CFU/mL to provide an instillation of 1.0×10^6 bacteria in 50 µL of physiological saline.

2.7.2. Mouse survival monitorings

After instillation, the mice were monitored and weighed every day until death or at the end of the experiment, *i.e.* 41 days. In agreement with the Remick laboratory report [44], mice were systematically euthanized when they reached the cutoff point, *i.e.* when they were found in a moribund state identified by the inability to maintain an upright position associated or not with labored breathing and cyanosis. Classical signs of distress, such as anorexia and weight loss (>20%), hunching, prostration, impaired motility, labored breathing, ruffled haircoat, and dehydration, were assessed. Mice exhibiting at least four of these criteria were euthanized via isoflurane (5%) anesthesia followed by cervical dislocation. Mice exhibiting less than four of these criteria were re-inspected each 8 h. Then, if the conditions of the mice worsened, they were euthanized. Surviving mice were used for detection of *Nocardia* cells at days 33 and 41. Survival curves (Kaplan–Meier plots) were compared by log rank test and performed on Prism8 software. P-values < 0.05 were considered statistically significant.

2.7.3. Detection and visualization of Nocardia cells among mouse organs

Organ histologic examinations were performed on the dead or euthanized mice. The inflammatory response and tissue damages due to *Nocardia* were evaluated at 4, 10, 33 and 41 days according to animal mortality curve due to animal ethical reasons linked to the concept of reduction (Fig. 2B). Small pieces of kidneys, spleen and liver were removed and fixed in formalin. For brain analysis and lung, the organs were removed and fixed by intratracheal infusion of paraformaldehyde (4%). They were kept in 4% paraformaldehyde for at least 36 h, dehydrated in successive baths with 30, 50 and 70% ethanol, embedded in paraffin, cut into 8 µm sections and stained with hematoxylin and eosin [45].

Crushed organs (lung, kidneys, brain, spleen and liver) diluted in 4.5 mL of a saline physiological solution, and serially diluted (10^{-1} to 10^{-4}) were used to estimate *Nocardia* plate count numbers. These plate counts were performed on BHI agar medium after a validation of the bacterial colonies using a *Nocardia*-specific PCR (NG1/NG2 primers (Table 1)). DNA extracts were produced from 200 µL of the above crushed organs using the NucleoSpin® Tissue kit (Macherey-Nagel, France). The *Nocardia*-specific PCR was then applied on these extracts to verify the presence of *Nocardia* cells in these organs.

3. Results

3.1. Spatio-temporal diversity of Nocardia cells in soils from an infiltration basin

Regarding physical–chemical parameters, soil water content of the SIS was quite variable between the three sampled areas and campaigns, varying from 9% in the upper zone in summer to saturation (155%) in the inflow zone in spring (Fig. 3). General trend was a higher moisture, at least 115%, in the inflow zone, and a lower water content, not higher than 56%, in the upper zone. Granulometry did not exhibit much variability between samples, with a relative mean sand content of 55–60% and a clay content of 40–45% (data not shown). Regarding metal trace elements, they have been shown to be constant over the time: Zn concentration remained around 0.5 mg/L and it was the highest concentration detected when comparing to other elements that respect the following relationship: Cd < Pb < Cu < Zn (data not shown). These pollutants were more abundant in the bottom zone than in the inflow and upper zones (p-value = 0.0195) (Fig. 4A). The PAHs, taken individually, harbored two clusterization patterns for 12 out of 16. So they were clustered according to the zone (fluoranthene, pyrene, phenanthrene, benzo(a)anthracene, benzo(a)pyrene, hereafter "5 PAHs") or the period of sampling (naphthalene, acenaphthene, fluorene, benzo(b)fluoranthene, dibenzo(a,h)anthracene, benzo(ghi)perylene, indeno(1,2,3-cd)pyrene, hereafter "7 PAHs"). The 4 remaining PAHs (acenaphthylene, anthracene, chrysene and benzo(k)fluoranthene) were not considered in this study because they don't exhibit any variability. The 5 PAHs were significantly more abundant in the inflow zone (p-value = 0.0157), while the 7 PAHs were significantly more abundant during the summer (p-value = 6.97×10^{-6}) (Fig. 4B & C).

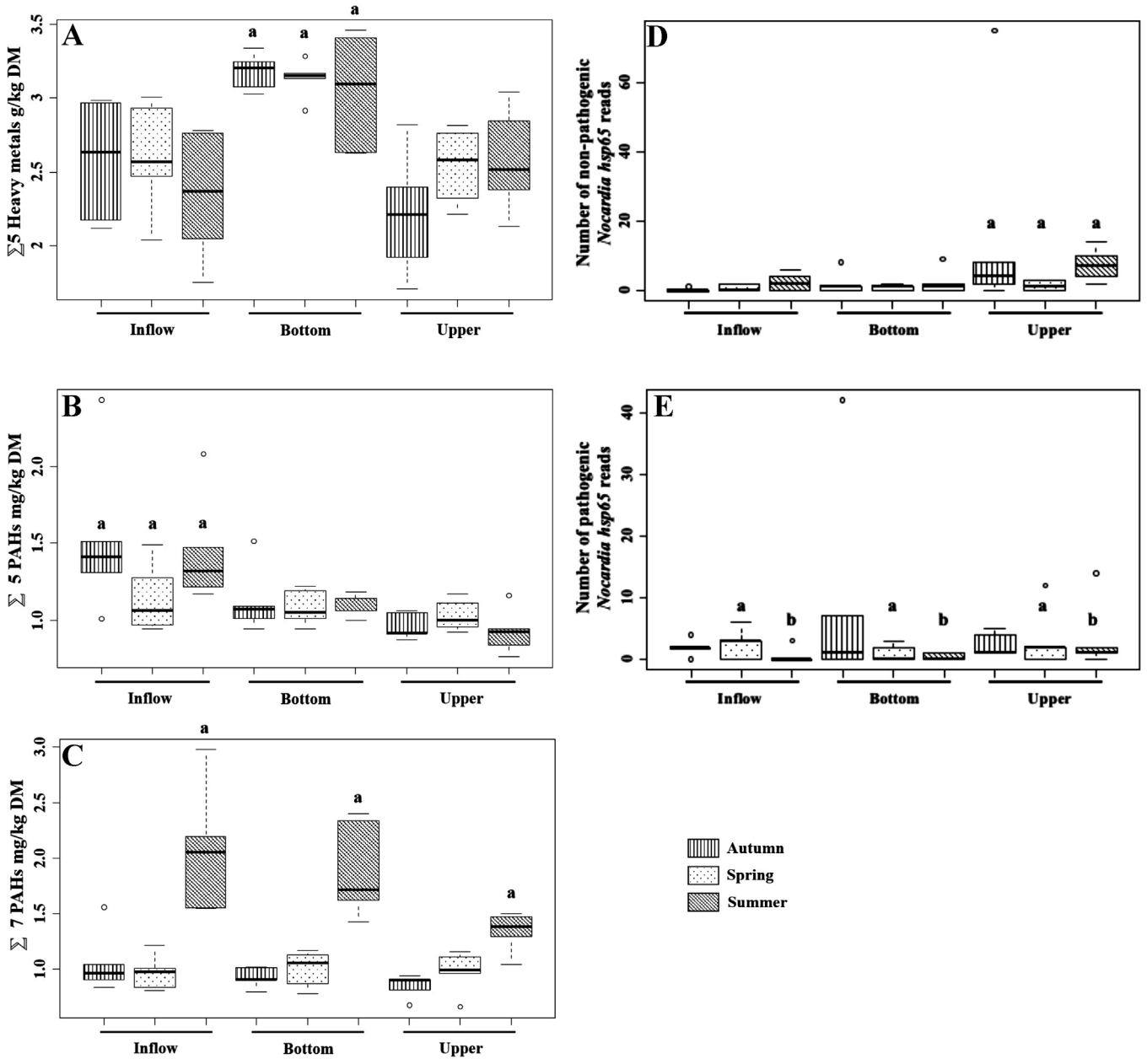

Fig. 4. Boxplots explicative of the between-class analysis (BCA). A. 5 trace element metals: Cd (Cadmium); Cu (Copper); Hg (Mercury); Pb (Lead) and Zn (Zinc). P-value a = 0.0195. B. 5 PAHs: fluoranthene, pyrene, phenanthrene, benzo(a)anthracene, benzo(a)pyrene. P-value a = 0.0157. C. 7 PAHs (polycyclic aromatic hydrocarbons): naphthalene, acenaphthene, fluorene, benzo(b)fluoranthene, dibenzo(a,h)anthracene, benzo(ghi)perylene, indeno(1,2,3-cd)pyrene. P-value a = 6.97x10-6. D. Non-pathogenic *Nocardia* species: *N. cummidelens, N. globerula, N. harenae, N. iowensis, N. jejuensis, N. pseudovaccinii, N. salmonicida, N. soli.* P-value a = 0.0294. E. Pathogenic *Nocardia* species: *N. abscessus, N. abscessus/asiatica, N. anaemiae, N. asteroides, N. brasiliensis, N. carnea, N. cerradoensis, N. cyriacigeorgica, N. ninae, N. nova, N. otitidiscaviarum, N. shimofusensis, N. sienata, N. vinaceae.* P-values a = 0.04055 and b = 0.02963.

DNA sequencing of the *hsp65* PCR products yielded good quality reads for each sediment sample (Table 3). Throughout the three sampling sites, the *hsp65* metabarcoding analytical scheme revealed a high diversity through the actinobacterial community according to Shannon index higher than 5 in all the samples except of SP2 in autumn (Table 3) and the Shannoneven index at 0.8 indicates that microbial populations are on evenness proportions. On a total of 320,760 reads allocated to the *Actinobacteria* class, 125,378 could not be allocated to a defined order. The *Mycobacterium* genus was the most abundant with 132,379 reads representing about 41.3% of the identified *Actinobacteria*, but 92,757 reads from this genus could not be allocated to a specific species within the *Mycobacterium* genus. Part of the most abundant *Mycobacterium* species were not pathogenic such as *M. neglectum* (31.8%) or *M. sediminis* (19.4%) but some others were opportunistic nontuberculous Mycobacteria (*M. doricum*: 22.7%, *M. fluoranthenivorans*: 2.1% or *M. manitobense*: 1.2%). The *Streptomyces* genus was another important group representing 2.7% of the identified *Actinobacteria* but no pathogenic species were recovered. *Gordonia* and *Nocardia* genus represented each about 0.4% and 0.2% of identified *Actinobacteria*, respectively.

The *hsp65* metabarcoding approach gave a more general view of *Nocardia* diversity in SIS allowing resolution to the species level (Fig. 3). Regarding the *Nocardia* community detected in the DRIB (Fig. 3), on the 507 *Nocardia* affiliated reads, only 203 reads could not be identified at the species level, indicating part of diversity

Table 3
Diversity and richness indices of the *hsp65* metabarcoding analysis.

Zone	Sample	Shannon Autumn	Shannon-even	Number of reads	Shannon Spring	Shannon-even	Number of reads	Shannon Summer	Shannon-even	Number of reads
Inflow	SP1	6.769454	0.850362	14,852	6.417540	0.809400	20,781	6.223242	0.789785	18,477
	SP2	4.599154	0.618105	20,279	5.138384	0.668644	21,826	6.114367	0.767870	20,255
	SP3	6.372891	0.806140	16,725	6.049869	0.776262	19,069	6.129255	0.782352	18,223
	SP4	6.451997	0.807211	17,855	6.105381	0.777861	19,702	5.597741	0.729251	16,189
	SP5	6.147986	0.787445	16,296	5.602082	0.741520	14,079	5.602386	0.734353	21,506
Bottom	SP6	5.862727	0.763773	15,311	6.324151	0.800348	15,733	6.416230	0.808466	20,265
	SP7	5.402151	0.710725	21,924	5.654639	0.731502	21,151	6.048270	0.769293	21,551
	SP8	6.374864	0.802821	19,138	6.418229	0.808028	17,795	6.207508	0.782555	22,832
	SP9	6.621081	0.835147	17,992	5.838846	0.752964	16,046	6.156486	0.778947	23,940
	SP10	6.360877	0.810332	19,628	6.180622	0.787997	15,732	6.580971	0.829486	16,981
Upper	SP11	6.597122	0.830997	19,100	6.246701	0.788356	18,921	7.194320	0.873336	25,995
	SP12	6.013042	0.764439	19,922	6.188532	0.779951	19,689	7.179103	0.877277	22,632
	SP13	6.879646	0.858737	17,783	6.350625	0.800308	19,069	7.185295	0.878364	24,621
	SP14	6.405939	0.807024	17,387	5.948913	0.754248	19,584	7.126191	0.873712	23,833
	SP15	6.636493	0.833514	17,664	6.278243	0.795136	17,258	6.496152	0.814367	24,676

Shannon is indicative of microbial community diversity whereas Shannoneven is indicative of the evenness proportion of different populations within the microbial community.

that still needs to be resolved. To confirm the accuracy of the Wang text-based Bayesian taxonomic classifications performed with MOTHUR [46], representative sequences of the *Nocardia hsp65*-OTUs were analyzed by BLASTn searches using the GenBank database. These searches confirmed all taxonomic inferences and showed that the unclassified sequences did not share enough identities to be clearly allocated to a particular species taking into account the chosen species identification criterion. However, even in these cases, closest results in terms of sequence similarity belonged to *Nocardia* genus. Hereafter, only reads allocated to well-defined species were analyzed and compared. A total of fourteen *Nocardia* species (relative abundance > 1%) could be tracked using the *hsp65* metabarcoding approach (Fig. 3). Most of these are opportunistic pathogens which also belong to the species the most clinically relevant in France (the classification of most/intermediate/less frequent pathogens was based on Lebeaux et al. [11]). In autumn, the most prevalent *Nocardia* species in the SIS (inflow, bottom, upper zones) were *N. cyriacigeorgica* and *N. nova* (clinically-relevant) together with *N. asteroides* and *N. cummidelens*. A segregation between zones was observed (Fig. 3). *N. cyriacigeorgica hsp65* reads were mainly observed in bottom zone (humidity rate = 72%) of the DRIB, while *N. nova* reads were mainly recovered from the inflow zone (water saturated samples). In spring, *N. asteroides hsp65* reads were observed in the three zones, and this species appeared to be the most prevalent in this environment. Reads from non-pathogenic *N. globerula* and the complex *N. abscessus/asiatica* (human pathogens) were also obtained in high numbers in the inflow and upper zones. In summer, most of the detected species were non-pathogenic ones: *N. globerula* showed the highest number of reads over the DRIB, but *N. salmonicida* (a fish pathogen) reads were higher in the inflow zone (see Fig. 3 for a summary of the taxonomic allocations).

Regarding the distribution of *hsp*65-OTUs per species, some were repeatedly observed from one campaign to another. Some *hsp*65-OTUs were found in multiple areas of the DRIB. Regarding *N. cyriacigeorgica*, which represents one of the species of most health concern for this genus, a total of 39 sequences was identified, representing 6 *hsp*65-OTUs. Most of these sequences (n = 36) were recovered from the bottom zone of the DRIB, but one sequence was recovered from the upper zone. Only one sequence of this species was recovered over two sampling campaigns.

Regarding the relative abundance of *Nocardia* species, they were clustered according to their potential health hazard or not. The pathogenic species are significantly less abundant in spring and in summer than in autumn and different between these two first seasons (p-values = 0.04066 for spring *vs* autumn and 0.02953 for summer *vs* autumn). The non-pathogenic species, *i.e.* not recognized as implicated in human nocardiosis, are most present in the upper zone than in the two others (p-value = 0.0294 for the upper zone *vs* inflow and bottom zones) (Fig. 4D & E).

When we compare both physical–chemical parameters and *Nocardia* relative abundance, we could see that there exists a clusterization according to the sampling areas. Humidity and 5 PAHs explained the clusterization in the inflow zone, while only non-pathogenic *Nocardia* species explained the clusterization in the upper zone. In the bottom zone, the explaining parameters were the pathogen *Nocardia* species, 7 PAHs, the soil granulometry and the heavy metals content (Fig. 5A & B).

The correlogram highlighted the potential correlation between metal trace elements and the relative abundance of non-pathogenic and pathogenic *Nocardia* species (Fig. 6). Indeed, a negative correlation was observed between the presence of zinc and mercury (p-value < 0.03) and the non-pathogenic species while there was a positive correlation between the presence of mercury and copper and pathogenic species. It could be also noted a negative correlation between the 7 PAHs and the relative abuncance of pathogenic species (p-value < 0.08).

To support the inferences made by the *hsp65* metabarcoding approach, attempts at isolating *N. cyriacigeorgica* strains from the DRIB sediment samples were performed. An averaged *N. cyriacigeorgica* plate count number of 1.0×10^3 CFU/g dry sediment was obtained (Fig. 1). From these platings, some isolates were purified, and twelve were confirmed to be *N. cyriacigeorgica* strains (by *rrs* and *hsp65* gene-based typing) and named DjR1 to 12 (2015–2016 isolates) and EML1456, already sequenced in Vautrin et al. [41] (Table 2). Several other species were also detected (*N. abscessus*, *N. nova*, *N. ignorata*, *N. asteroides*, *N. salmonicida*, etc.) but out of scope in this study. The DjRm12-14 are sequences identified according to the metabarcoding analysis on the sampled sediments of the DRIB (2015–2016). Location of these SIS isolate community and sequences over the DRIB is indicated on Fig. 1. Deeper taxonomic allocations of these strains by phylogenetic analysis are shown below.

3.2. Phylogenetic relatedness of SIS and clinical isolates

To go deeper into the evaluation of health hazards that can be associated with SIS *N. cyriacigeorgica* isolates, we obtained the phylogenetic trees built from individual locus and concatenated

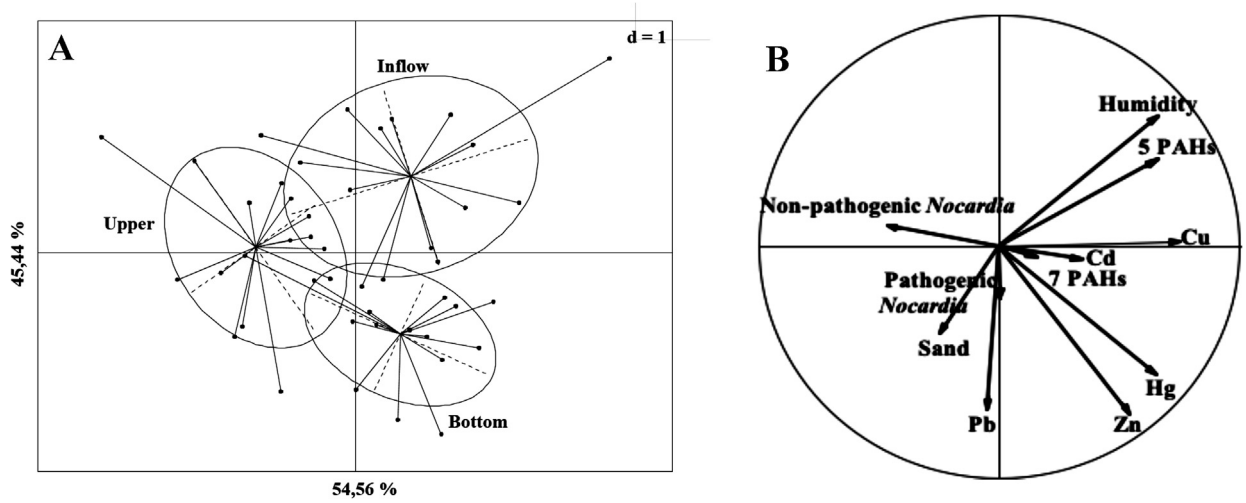

Fig. 5. A. Between-Class Analysis (BCA) performed on physical–chemical parameters and *Nocardia* relative abundance from sediments of the Django-Reinhardt infiltration basin (DRIB). B. Explicative factors of the BCA. 7 PAHs (polycyclic aromatic hydrocarbons): naphthalene, acenaphthene, fluorene, benzo(b)fluoranthene, dibenzo(a,h) anthracene, benzo(ghi)perylene, indeno(1,2,3-cd)pyrene ; 5 PAHs: fluoranthene, pyrene, phenanthrene, benzo(a)anthracene, benzo(a)pyrene; Cd (Cadmium); Cu (Copper); Hg (Mercury); Pb (Lead) and Zn (Zinc). Pathogenic *Nocardia* species: *N. abscessus, N. abscessus/asiatica, N. anaemiae, N. asteroides, N. brasiliensis, N. carnea, N. cerradoensis, N. cyriacigeorgica, N. ninae, N. nova, N. otitidiscaviarum, N. shimofusensis, N. sienata, N. vinaceae* ; non-pathogenic *Nocardia* species: *N. cummidelens, N. globerula, N. harenae, N. iowensis, N. jejuensis, N. pseudovaccinii, N. salmonicida, N. soli.*

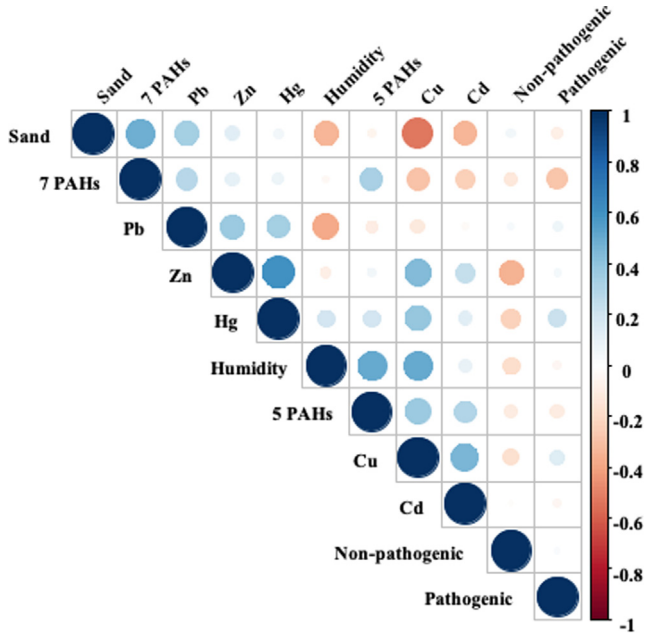

Fig. 6. Correlogram of the physical–chemical parameters and *Nocardia* pathogenic and non-pathogenic species relative abundance. 7 PAHs (polycyclic aromatic hydrocarbons): naphthalene, acenaphthene, fluorene, benzo(b)fluoranthene, dibenzo(a,h)anthracene, benzo(ghi)perylene, indeno(1,2,3-cd)pyrene ; 5 PAHs: fluoranthene, pyrene, phenanthrene, benzo(a)anthracene, benzo(a)pyrene; trace element metals: Cd (Cadmium); Cu (Copper); Hg (Mercury); Pb (Lead) and Zn (Zinc).

genetic loci (*rrs, hsp65, sodA*, *secA1*) (Fig. 7). The phylogenetic tree based on *rrs* gene grouped all the clinical and environmental *N. cyriacigeorgica* strains into a single phylogroup (data not shown). The phylogenetic tree obtained from *hsp65* gene sequences of the analyzed strains in this work showed a distribution into three significant phylogroups (PI, PII and PIII) that matched previous groups defined by Schlaberg et al. [9]. Thanks to some sequences representatives from the metabarcoding analysis and integrated in *hsp65*-tree, we could observe that different genotypes were splited onto two different *hsp65*-phylogroups (I and III) for *N. cyriacigeorgica* species (Fig. 7A: DjRm sequences only). Phylogroup I (PI) harbored the *N. cyriacigeorgica* type strain *hsp65* sequence, environmental sequences obtained from the metabarcoding analysis (DjRm.12 and DjRm.14) and French clinical strains, including one belonging to a patient from Lyon, which was a resident in the geographic area of the DRIB. This phylogroup can be seen as a clonal complex as it encompassed 5 different OTUs issued from the metabarcoding analysis. Phylogroup II (PII) harbored clinical strains including GUH-2. Phylogroup III (PIII) also harbored environmental sequences obtained from the metabarcoding analysis (DjRm.13, SIS *N. cyriacigeorgica* isolates (EML446, DjR.1 and DjR9) and clinical strains. Only 1 OTU joined this phylogroup. Bootstrap values were > 80 only for PI (85] and PIII (98) (Fig. 7a).

For *sodA* and *secA1*, the phylogenetic tree structures were in agreement with the one derived from *hsp65* gene (data not shown). The MLSA phylogenetic tree of concatenated gene sequences increased the reliability of the groupings (Fig. 7B). This tree better resolved the relatedness of the SIS isolates with the clinical strains. Low infra-specific divergences were observed within PI (similarity mean = 99.7%, min–max = 99.4–100%) and PII (similarity mean = 99.8%, min–max = 99.6–100%). In PIII, infra-specific divergences were higher (mean identities = 99.5%, min–max = 99.2%-100%) (Supplementary Table 1). However, only PI and PIII clustered clinical and environmental strains, instead of PII that clusters only clinical strains. The MLSA tree showed a clear phylogroups distribution harboring SIS and also clinical strains from the French Observatory of Nocardiosis. These phylogroups that matched those of *hsp*65 ones. So, in the same way as for *hsp*65 tree, we can state that MLSA-phylogroup I represent a clonal complex inside *N. cyriacigeorgica* species.

3.3. EML 446 and GUH-2 genome comparisons

The whole genome sequencing (WGS) of DRIB *N. cyriacigeorgica* EML446 (MLSA-PIII) resulted in the obtaining of 41 contigs that could be assembled into a circular chromosome of 6,530,670 bp with a G + C content of 68.21%. This genome encodes 51 tRNA, 3 rRNA and 6,230 CDSs (coding sequences). Analysis on the MicroScope platform with the Virulome tool highlighted the presence of

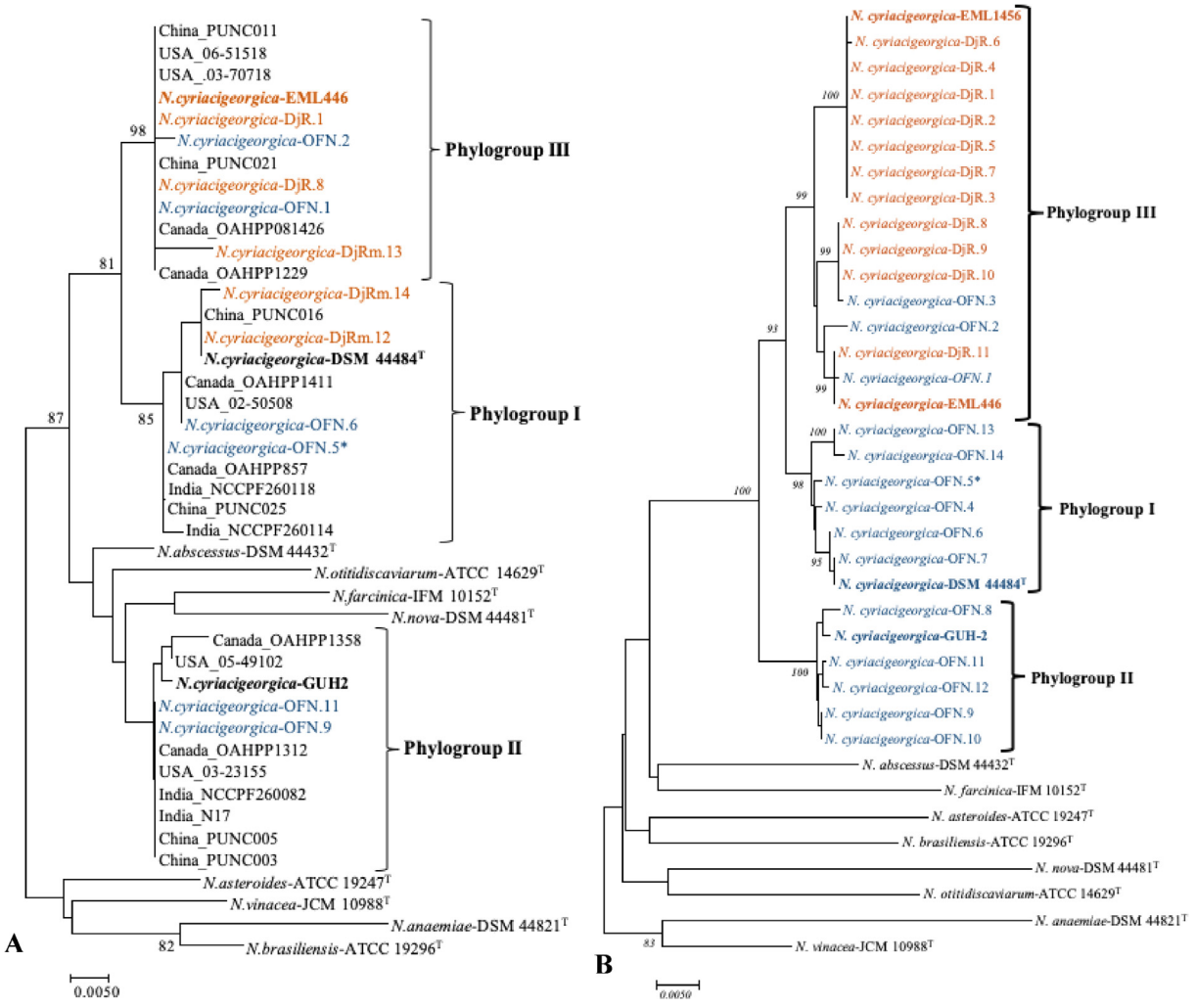

Fig. 7. Molecular phylogeny of *Nocardia cyriacigeorgica*. A) Unrooted phylogenetic tree based on the *hsp65* sequences (401 bp) from USA [9], Canada [35], India [36] and China [37] isolates, and representative *N. cyriacigeorgica* sequences from the metabarcoding analysis, and the clinical and SIS strains reported in this study. OFN.5* corresponds to a patient from Lyon (France). DjR.1, DjR.8 and EML446 corresponding *hsp65* sequences were used to represent the environmental cluster. B) Unrooted phylogenetic tree based on the *rrs-hsp65-sodA-secA1* concatenated sequences (1,845 bp). The maximum likelihood tree was constructed using MEGA software (version 7.0.16) after having aligned the sequences with ClustalW. The bootstrap values were calculated from 1,000 replicates, and those higher than 80% are given at the corresponding nodes. Clinical strains are colored in blue, and environmental strains are colored in orange. (For interpretation of the references to color in this figure legend, the reader is referred to the web version of this article.)

130 CDSs (*i.e.* 2.09% of the CDSs) that can be involved in virulence in EML446 (MLSA-PIII) while 108 CDSs involved in virulence were found among GUH-2 (MLSA-PII), the model strain to investigate virulence in *Nocardia*. Among these CDSs, 96 were found to be in common. A Venn diagram was drawn to highlight the number of shared CDSs between *N. cyriacigeorgica* EML446 (MLSA-PIII), GUH-2 (MLSA-PII) and DSM 44484 ^{T} (MLSA-PI), and *N. farcinica* IFM 10152^{T} and *M. tuberculosis* H37Rv (Fig. 8a). The EML446 genome shared 4,392 CDSs with GUH-2 and 4,883 with DSM 44484 ^{T}. GUH-2 and DSM 44484 ^{T} shared 4,408 CDSs, and the number of shared CDSs between any *N. cyriacigeorgica* strain and *N. farcinica* IFM 10152 ^{T} or *M. tuberculosis* H37Rv was lower. Comparison of 11 gene families between these genomes did not show many differences except for polyketide synthase (27 for *M. tuberculosis* compared to 7 for the three *Nocardia* genomes), lipoproteins (62 compared to 7–16) and PE_PGRS ((proline-glutamic acid_polymorphic guanine-cytosine-rich sequence) 62 compared to 0–1). Only the NRPS (nonribosomal peptides synthetases) CDSs were lower for *Mycobacterium*, having 3 compared to 14–17 for *Nocardia* (Table 4). According to these analyses, the EML446 strain from the UIB polluted sediments has the genetic potential to be as virulent as the *N. cyriacigeorgica* GUH-2 clinical isolates. On the other hand, the MAUVE analysis highlights a decrease in CDSs content in the region of genomic plasticity (RGP) between the two genomes *N. cyriacigeorgica* EML446 and GUH-2 (Fig. 8b)

3.4. Pathophysiology of N. cyriacigeorgica in a murine model of transient immunoparalysis

In the present study, 37% of the CLP-operated mice died prior to the instillation step (37/101) in accordance with the model of septic immunoparalysis established by Restagno et al. [43]. Five days after the first hit, *i.e.* the CLP operation, Sham and CLP-operated mice were randomized as described in Figs. 2A and 2B.

The survival results showed a survival rate of 100% after 41 days for Sham-NaCl and CLP-NaCl groups. For mice intratracheally instilled by a load of *Nocardia* at 1.0 × 10^{6} CFU/mouse, Sham-EML446 showed the same survival rate (Fig. 9). In the Sham-GUH-2 group, only one mouse died at D6 (survival rate = 86% (6/7 mice)). For both the CLP-GUH-2 and CLP-EML446 groups, during the first 10 days following intratracheal bacterial challenges, the survival rates were not statistically different (p-value = 0.36):

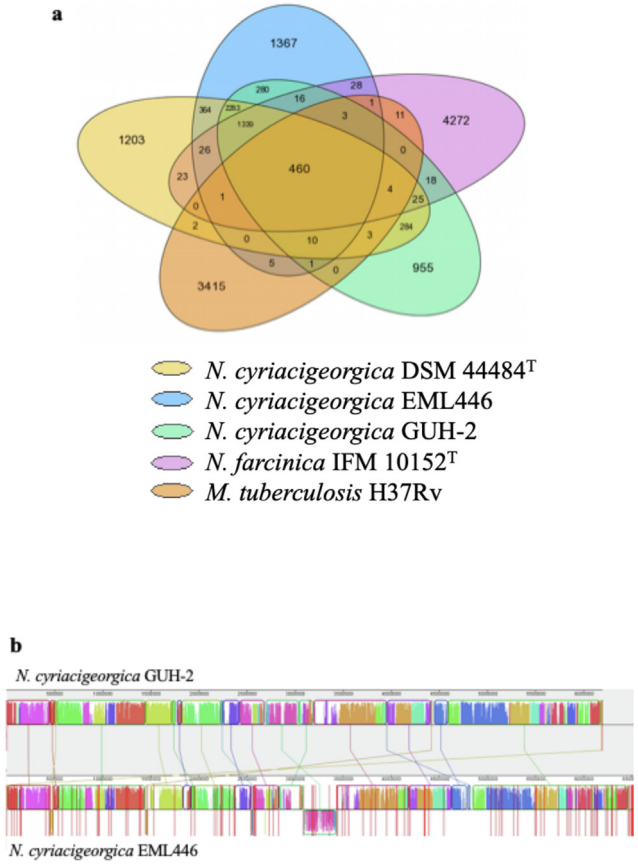

Fig. 8. Comparison of *Nocardia cyriacigeorgica* EML446 genome with other actinomycetal reference genomes. (a) Venn Diagram representing the number of shared CDSs between whole genomes of *N. cyriacigeorgica* DSM 44484^T, *N. cyriacigeorgica* EML446, *N. cyriacigeorgica* GUH-2, *N. farcinica* IFM 10152^T and *Mycobacterium tuberculosis* H37Rv. (b) MAUVE comparison between EML446 and GUH-2 genomes showing the position of RGPs (regions of genomic plasticity).

CLP-GUH-2, survival 67% (6/9 mice) and CLP-EML446, survival 64% (7/11 mice). A second episode of mortality occurred at 30 days for CLP-GUH-2, decreasing the survival rate at 44% (4/9 mice). As compared to respective sham groups survival decreased significantly for CLP-GUH2 (p-value = 0.02) and CLP-EML446 (p-value = 0.04) groups.

The TCBD (time course bacterial detection) experiment showed that in the Sham-operated group, soon after intratracheal instillation, the lung was the primary infection site of *Nocardia*, but other organs were also affected. At D4, 4/5 Sham-GUH-2 mice presented *Nocardia* in the lungs; in two of them, *Nocardia* was detected in all the studied organs (Table 5). Only in one mouse, *Nocardia* could not be detected. At D10 and D33, the number of organs positive for *Nocardia* decreased except in the lungs (2/3 mice at D10 and 3/4 mice at D33) and kidneys (1/3 at D10 and 3/4 at D33). For the Sham-EML446 mice, the occurrence rate and dissemination were lower than for the Sham-GUH-2 mice. At D4, *Nocardia* was found in the lungs of 3/5 mice, but the incidence in other organs was lower (1/5) and even null in the brain and spleen. At D10, only 1/5 mice presented *Nocardia* in each organ, and nothing was detected at D33. However, *Nocardia* was found in all organs of one mouse at D41.

In the CLP-operated group, at D4, the presence of *Nocardia* was observed in all of the inspected lungs for both strains (5/5 for CLP-GUH-2 and 6/6 for CLP-EML446), but it was almost missing in the other organs (only in 3/5 CLP-GUH-2 and 2/7 CLP-EML446 in the kidneys). At D10, 100% of the inspected lungs were still positive for *Nocardia,* and all the other organs became progressively positive: 3/5 (CLP-GUH-2) and 4/4 (CLP-EML446) positive in the kidneys, 4/5 (CLP-GUH-2) and 3/4 (CLP-EML446) positive in the brains and spleens, 3/5 (CLP-GUH-2) and 3/4 (CLP-EML446) positive in the livers. At D33, the presence of *Nocardia* in the lungs remained especially high for CLP-GUH-2 mice (7/8) but relatively low for CLP-EML446 mice (2/5). Dissemination in other organs was almost similar for both strains excepting for the liver. At D41, almost all the organs of CLP-EML446 mice were positive at high rates (Table 5). As expected, no NaCl-operated mice (controls) showed *Nocardia* cells in their organs.

In the lungs of CLP-EML446 mice (1/1), histological signs of pneumonia similar to nocardiosis were clearly observed, as histologic pictures showed multiple cavity lesions at D4 (Fig. 10A & B). A strong mononuclear infiltrate in the periphery of the microabscesses among the collagen fibers was also observed (Fig. 10A1, A2 & B3). The presence of numerous filamentous bacteria in the caseous necrosis area suggests that these granulomatous lesions were infectious and that the mice developed nocardiosis (Fig. 10B). At D41, 1/3 CLP-EML446 mice exhibited mild pneumonia (Fig. 10C). Nothing was observed at D41 in Sham-EML446 mice (0/2) (Fig. 10D). As expected, no histological lesions in any organ were observed for Sham-NaCl (n = 2 at day 41) or CLP-NaCl (n = 2–3 at D4, D10, D33 and n = 6 at D41) mice. No lesions were found in the brains of CLP-EML446 mice at D41 (n = 2). No specific nocardiosis lesions were found in other organs (kidney, spleen, liver) at D4, D10, D33 of either Sham-EML446 (n = 2/organ) or CLP-EML446 (n = 2/organ) mice. At D41, no specific nocardiosis lesions were

Table 4
Number of virulence CDSs (coding sequences) per functional categories shared between *N. cyriacigeorgica* GUH-2, EML446 and two other pathogenic species *N. farcinica* IFM 10152^T and *Mycobacterium tuberculosis* H37Rv:

Virulence CDSs	*N. cyriacigeorgica* EML446	*N. cyriacigeorgica* GUH-2	*N. farcinica* IFM10152^T	*M. tuberculosis* H37Rv
PKS (polyketide synthase)	7	7	7	27
NRPS (nonribosomal peptides synthetases)	17	17	14	3
Lipoproteins (Lpps)	16	17	7	62
Hemolysin	2	2	2	2
Esterases	18	17	24	15
PE_PGRS (proline-glutamic acid_polymorphic guanine-cytosine-rich sequence)	1	1	0	62
sod (superoxide dismutase)	2	2	2	2
mce (mammalian cell entry	6	6	7	4
cat (catalase)	3	3	3	1
narBGHIJK (nitrate reductase)	6	6	5	6
nirBD (nitrite reductase)	2	2	2	2

Note: number of genes were found by keyword search tool on the MicroScope platform (http://www.genoscope.cns.fr/agc/microscope/). Virulence genes were selected according to [42].

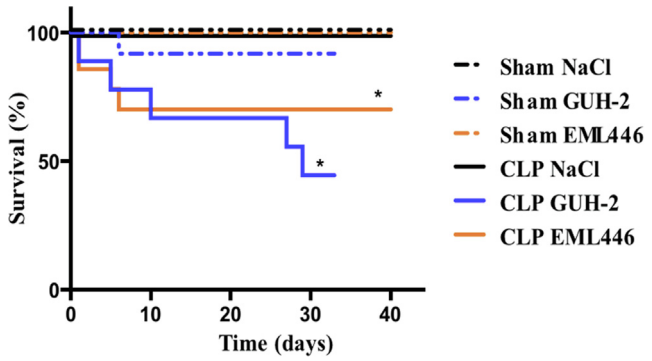

Fig. 9. Survival rate after *N. cyriacigeorgica* cells instillations of Sham and CLP mice. Five days post-CLP (*i.e.* D0), mice were challenged with an intratracheal administration of *Nocardia* GUH-2 or EML446 at 1.0×10^6 CFU/mouse. Either NaCl (physiological saline solution) (Sham n = 7, CLP n = 7), GUH-2 (Sham n = 7, CLP n = 9) or EML446 (Sham n = 5, CLP n = 11) were instilled. Results are expressed as Kaplan-Meier survival curves. * p-value < 0.05 was considered statistically significant compared to the respective control groups.

found in kidney, spleen, liver of Sham-EML446 (n = 5/organ) mice, but small granulomas were observed in the livers of 5 CLP-EML446 (n = 7/organ) mice (Fig. 10E).

4. Discussion

The dissemination of hazardous biological agents in cities, outside hospital settings, remain largely under explored. Urban soils and waters can offer shelters for some pathogenic micro-organisms such as the opportunistic ones. With their increasing contact with human populations, these pathogens might be undergoing selective processes that will make them better fit for a colonization of the human host. Furthermore, urban chemical pollutants seem to generate a "dangerous liaison" with these micro-organisms as demonstrated by Cui et al. [47] who found the presence of 16 bacterial genera harboring pathogenic species such as *Aeromonas* and *Mycobacterium* in polluted lakes in an industrial area in China. Furthermore, Fan et al. [48] showed a relation between concentrations of chemical pollutants and airborne pathogenic bacteria in air samples. Regarding *Nocardia*, also, some authors have already described a potential relationship between organic pollutants and presence of *Nocardia*. As explained by Arrache et al. [49] this relationship could explain the infective source associated to a case of cerebral nocardiosis of an immunocompetent individual exposed to the inhalation during a long period of time of dusts rich in hydrocarbons in a refinery which probably hosted the *Nocardia cyriacigeorgica* species responsible of his pathology.

Nocardia are known to be widely spread among outdoor environments but several species represent a public health concern. This genus includes opportunistic pathogens that primarily cause pulmonary infection following inhalation [50,51]. These species can cause pulmonary nocardiosis in immunocompromised individuals associated with high-dose corticosteroids treatments [51,52]. Non-immunocompromised patients like cigarette smokers, or those affected by bronchiectasis and acute bronchitis, and other chronical pulmonary diseases, are also at risk of pulmonary nocardiosis. These clinical pictures affect about 60 million people around the world, according to the WHO, and are often related to high atmospheric pollution including high content in aerosolized dusts. These dusts can be generated by several urban components such as motor engines, chemical industries, garbage incinerators, stored garbage on sidewalks, plant and animal detritus, etc. They are accumulating on urban surfaces and washed away with the runoff waters during rain events or aerosolized. Polluted urban runoffs are nowadays transferred either to wastewater treatment plants (WWTP), SIS, or natural waterways. These washed urban sedi-

Table 5
Heatmap representing rates of contaminated mice by *N. cyriacigeorgica* and detected with specific *Nocardia*-genus PCR. Mice were sacrificed 4, 10 and 33 days after instillation for the GUH-2 strain and until 41 days for the EML446 strain. Lungs, brain, kidneys, spleen and liver were sampled for *Nocardia* detection. Clinical strain GUH-2 is colored in blue, and environmental EML446 is colored in orange. The deeper is the color, the more contaminated are the mice. The heatmap only reveals the presence or absence of *Nocardia* but is not quantitative. [H] *some organs were used for histological analysis and were not available for bacterial detection since it is not technically possible to do both.* [n=x] *corresponds to the number of mice reserved for histological analysis.*

		Lungs	Kidneys	Brain	Spleen	Liver
Sham-GUH-2	4 days	4/5	2/5	2/5	2/5	2/5
	10 days	2/3	1/3	0/3	0/3	0/3
	33 days	3/4	3/4	1/4	2/4	0/4
Sham EML446	4 days	3/5	1/5	0/5	0/5	1/5
	10 days	1/5	1/5	1/5	1/5	1/5
	33 days	0/2	0/2	0/2	0/2	0/2
	41 days	1/3 [H n=2]	1/5	1/5	1/5	1/5
CLP GUH-2	4 days	5/5	3/5	0/5	0/5	0/5
	10 days	5/5	3/5	4/5	4/5	3/5
	33 days	7/8	4/8	4/8	3/8	0/8
CLP EML446	4 days	6/6 [H n=1]	2/7	0/7	0/7	0/7
	10 days	4/4	4/4	3/4	3/4	3/4
	33 days	2/5	3/5	3/5	2/5	3/5
	41 days	4/4 [H n=3]	7/7	4/5 [H n=2]	7/7	6/7

GUH-2	EML446
0 – 19 %	0 – 19 %
20 – 39 %	20 – 39 %
40 – 59 %	40 – 59 %
60 – 79 %	60 – 79 %
80 – 100 %	80 – 100 %

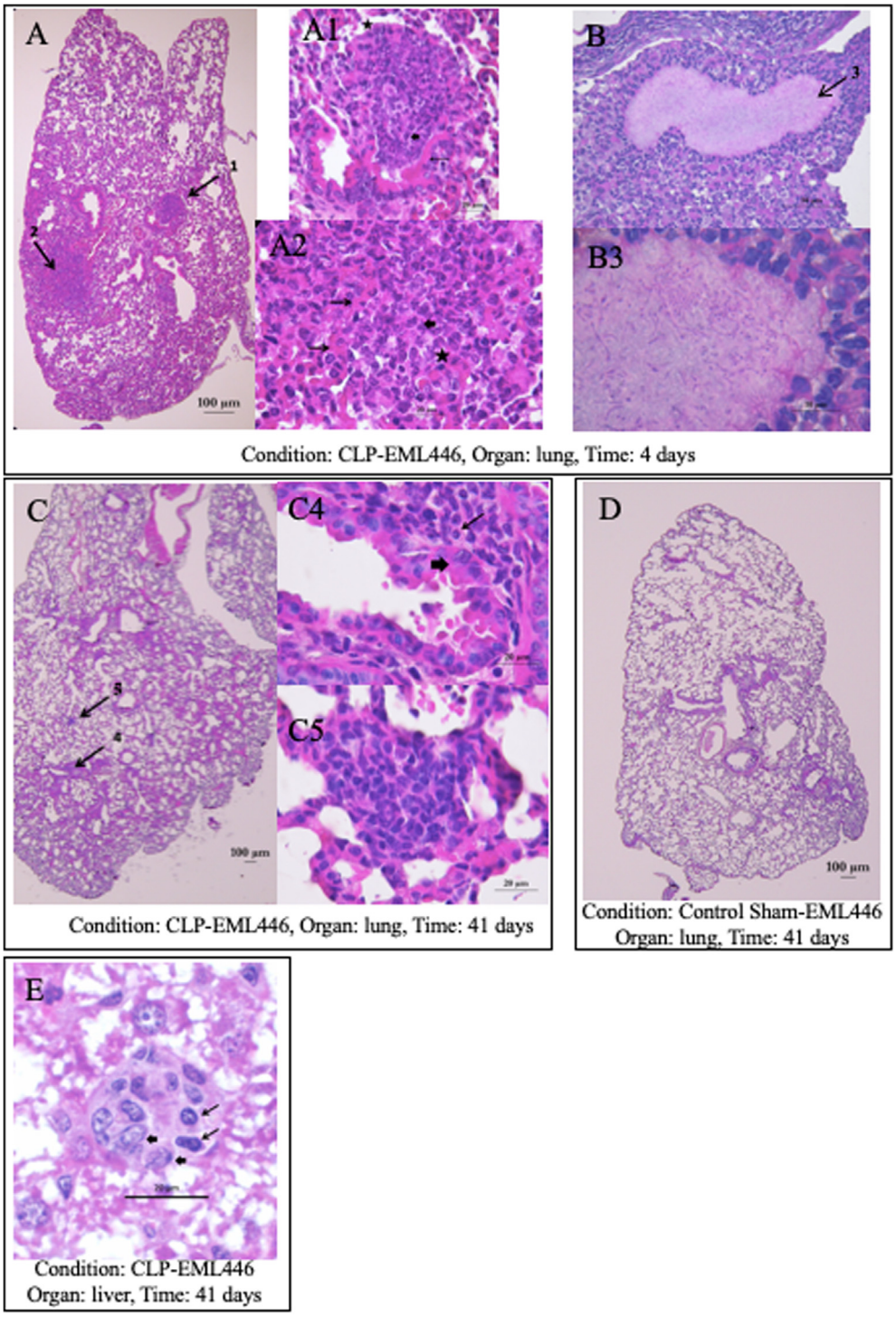

Fig. 10. Histological lung and liver sections of CLP-EML446 mouse at days 4 and 41 after intratracheal instillation. A, B: CLP-EML446 mouse lung at day 4. Light micrographs of mouse lung section with evidence of granulomatous process characterized by both inflammatory response (A) and necrosis usually present in nocardiosis (B). A: Two early pyogranulomas disseminated in the pulmonary parenchyma (arrows). Original magnification: obj. 4×, lungs, postcaval lobe. A1: enlargement of the pyogranulomas (arrow 1). Multiple degenerated neutrophilic polymorphonuclear cells into a lung alveolus lumen admixed with few macrophages. Some inflammatory cells overflow in the lumen of a bronchus. Thin arrow: bronchus epithelium. Large arrow: neutrophilic polymorphonuclear cells. Star: macrophages. Original magnification: obj. 40 X. A2: enlargement of the pyogranulomas (arrow 2). Multiple degenerated neutrophilic polymorphonuclear cells into a lung alveolus lumen admixed with few macrophages. Thin arrows: alveolar wall. Large arrow: neutrophilic polymorphonuclear cells. Star: macrophages. Original magnification: obj. 40 X. B: The lungs showed cavitary lesions constituted by central necrotic material surrounded by some polymorphonuclear and numerous macrophages. Macrophage alveolitis and interstitial lymphocytic infiltration are also observed. Light micrographs; hematoxylin–eosin staining; original magnification: obj. 40 X. B3: High power magnification showing histologic sections of the lesion characterized by caseous necrotic central area with filamentous bacteria inside. Light micrographs; hematoxylin–eosin staining; original magnification: obj. 100 X. C: CLP-EML446 mouse lung at day 41: C: At day 41, some lymphocyte aggregates are present in the interstitium (arrows). Original magnification: obj. 4×, lungs, postcaval lobe. C4: enlargement of the aggregate (arrow 4). Some small lymphocytes (thin arrow) infiltrate the interstitium beneath the bronchial epithelium (large arrow). Original magnification: obj. 100 X. C5: enlargement of the aggregate (arrow 5). Some small lymphocytes infiltrate the interstitium of the interalveolar wall. Original magnification: obj. 100 X. D: Sham EML446 mouse lung at day 41. no lesions. Original magnification obj. 4×, lungs, postcaval lobe. E: CLP-EML446 mouse liver at day 41. Mature granuloma disseminated at random into liver lobules. Thin arrows: lymphocytes. Large arrows: macrophages. Original magnification obj. 100×.

ments can thus create novel growth conditions for opportunistic human pathogens that are known to be well-adapted for a growth on chemical pollutants. Results obtained in this study supported this hypothesis as high numbers of *N. cyriacigeorgica* cells were observed among SIS sediments, and these cells were allocated to a MLSA-phylogroup harboring clinical strains that had been involved in lung infections. Other pathogenic *Nocardia* species such as *N. abscessus* (associated mainly with cerebral and pulmonary infections), *N. nova* (related with pulmonary and cutaneous cases), and *N. otitidiscaviarum* (causing mainly cerebral infections and multidrug resistant) were also identified among SIS through the use of a novel metabarcoding approach based on the *hsp65* gene target. These species can thus also be disseminated through SIS and aerosolized deposits.

Sediments analyzed from the DRIB showed variable water contents, high hydrocarbon pollution and variable plant cover. The main pollution recorded in this urban environment is due to PAHs. The high amount of PAHs has a pyrogenic origin according to the phenanthrene/anthracene < 10 and fluoranthene/pyrene > 1 ratio for all the samples in accordance with Budzinski et al. [53] and Yunker et al. [54]. This pyrogenic origin could be explained by the industrial activity in this area and the engine gasoline combustion. No petrogenic origin could be identified in this study, contrary to Marti et al. [16] that reported a petrogenic origin for most of the PAHs in the detention basin upstream the infiltration basin, indicating a good performance in removing oils from water and avoiding the plugging of the infiltration basin. Nadudvari & Fabianska [55] reported a pyrogenic origin in sediments in a river in Poland arising from runoff water and city waste combustion. The same phenomenon was first described by Radke & Welte [56] in oil wells in Canada. Five of the detected PAHs (phenanthrene, fluoranthene, pyrene, benzo(a)anthracene and benzo(a)pyrene) were already reported by Sebastian et al. [14] in the same DRIB as being specially more abundant for the inflow zone which is confirmed by our study. On the other side, we observed a group of 7 PAHs (naphthalene, acenaphthene, fluorene, benzo(b)fluoranthene, dibenzo (a,h)anthracene, benzo(ghi)perylene, indeno(1,2,3-cd)pyrene) that are more abundant in summer regardless the measured zone which agrees with the study of Belles et al. (2016) also in the same studied system. Regarding the correlation between pollutants and relative abundancy of *Nocardia*, this high amount of PAHs seems to inhibit the development of *Nocardia* species, while metal trace elements can be an explicative factor of pathogenic species presence in the bottom zone of this infiltration basin. Regarding the influence of PAHs in pathogenic *Nocardia*, the upper zone, considered as the less contaminated zone, was the one with lowest counts in *N. cyriacigeorgica*. So, we could consider that upper zones represent a low risk of infection by aerial pathway as respiratory infections are the most usual in nocardiosis. However, other pathways should not be excluded (*e.g.* direct contact with water, transmission to phreatic zone below, etc.). Moreover the persistence of pathogenic *Nocardia* in humid areas could be seen as a reservoir as it could be transmitted by aerosolization in eventually favorable environmental conditions (*e.g.* dryer period).

Hsp65-based metabarcoding revealed as a powerful tool in the identification at species level of *Actinobacteria* but showed some limitations evidenced by the number of reads that could not be assigned to this class. This may be possibly due to the lack of *hsp65* sequences in used database for many *Actinobacteria* taxa. However, obtained results from this *hsp65* metabarcoding analysis concerning species-level *Nocardia* taxa, showed that water content was found to be explicative of some distribution patterns. Shannon indices highlighted a high diversity within the sampled sediments but similar values could indicate a low variability between the samples in a same area. The lower diversity within the SP2 sample in autumn (according to its Shannon index) could be explained by the fact that this sample point was the one with the highest humidity rate among those of the other sample points of the inflow area (max humidity $\geq$ 115%). Extremely high humidity rates may favor the development of few bacterial communities detrimental to others. In this study, we observed that a high water content ($\geq$112%) was related to the higher number of *N. abscessus* and *N. nova hsp65* reads, and intermediate conditions (around 72% sediment moisture) led to the higher number of *N. cyriacigeorgica hsp65* reads. Most of the species found with the metabarcoding tool were also detected by cultural method reinforcing the validity of this first approach. However, no quantification nor comparison of the accuracy of these techniques was in the scope of this work.

These observations suggest *N. cyriacigeorgica* to be the most worrisome species as its environmental conditions for isolation are those present the most part of the year in the studied system and besides, according to Zoropogui et al. [42] this species presents a likely ongoing evolution towards a higher tropism for the human host. This led us to further investigate the SIS *N. cyriacigeorgica* isolates. The phylogenetical analysis demonstrated close relationships between the clinical and some of the SIS *N. cyriacigeorgica* of this study. Moreover, a recent clinical strain from a patient living in the Lyon area was also positioned in one of the MLSA-phylogroups harboring SIS's *N. cyriacigeorgica* strains, allowing us to wonder of the source of infection of this person. In fact, clinical strains and environmental ones could not be segregated into distinct clusters. This supports the idea that all strains of *N. cyriacigeorgica* represent a human health hazard. Direct exposures through inhalation could thus result in pulmonary nocardiosis. However, the degree of exposure with the human host could have generated a gradient of virulence potentialities going from mild to severe. This hypothesis was verified with the results of the genomic and '*in vivo*' comparison of GUH-2 and EML446 strains.

Regarding the genomic analysis, the genome size of SIS *N. cyriacigeorgica* EML446 (6,530,670 bp) was found to be larger than the one of clinical GUH-2 (6,194,645 bp). In general, opportunistic pathogens present in an environmental reservoir harbor a larger genome, conferring a greater versatility in the use of nutrients and in the ability to resist at certain environmental constraints [57]. However, the differences in genome size between EML446 and clinical GUH-2 are low, and not in favor of a size reduction related to greater interactions with the human host. Furthermore, the content in virulence genes between these strains did not differ substantially but its distribution is variable in both genomes. Indeed, Zoropogui et al. [42] had already demonstrated that part of the virulence genes of clinical GUH-2 strain is contained in the RGPs (region of genomic plasticity) (Fig. 8b). In fact, several CDSs found in *N. cyriacigeorgica* EML446 could play part in lung colonization. For example, *mbt* is involved in the development of slow-growing bacteria in tissues under iron limitations, *e.g.* in the lung [58]. In addition, the presence of CDSs coding for lipoproteins may contribute at the intracellular lifestyle of *N. cyriacigeorgica*. Actually, Li et al. [59] demonstrated that a large amount of lipoproteins improves survival of another actinobacteria, *Mycobacterium smegmatis*, in macrophage cells and murine lungs. Finally, CDSs such as PE_PGRS30, PG_PGRS33 and PE_PGRS41, were shown to be essential for entry and intracellular survival in macrophages. These virulence genes were also recorded in clinical *N. cyriacigeorgica* GUH-2 strain. This suggests that virulence of these two strains on a mouse model (or in human) should be similar.

Anyway, our work focused in a limited number of virulence genes [42] so, it would be interesting further complete virulome studies including more genomes from other *Nocardia* species and from other pathogenic microorganisms in order to obtain more information about the genetic factors of the virulence in *Nocardia*.

However, changes in regulatory pathways might have generated some changes in the fine-tuning of the expression of virulence

genes, and modified the clinical outcomes. This is hardly detected by simple genomic comparisons, and would require gene expression profile analyses as performed by Cruz-Rabadán et al. [60]. Nevertheless, it must be noted that the GUH-2 MLSA-phylogroup (PII) diverged from the EML446 MLSA-phylogroup (PIII), suggesting adaptation and selection for distinct context (human *vs* environment). This on-going adaptation of the GUH-2 lineage is certainly due to repeated passed through humans, and this hypothesis thus needed to be studied.

The pathophysiology of *N. cyriacigeorgica* has been extensively studied in immunocompetent murine models [9]. However, nocardiosis has a higher occurrence in immunocompromised patients, and this led us to use a transient immunoparalysis (induced by mild CLP) mouse model to compare the virulence potentialities of GUH-2 and EML446. This is the first report describing the use of this model system with *Nocardia* cells, but previous validations had been performed with *P. aeruginosa* cells [44]. Compared on this latter study, our *Nocardia* cell instillations at 1.0×10^6 CFU/ CLP mouse led to a lower survival at D8 (CLP-EML446 = 64%, CLP-GUH2 = 67%) than the one obtained with *P. aeruginosa* at the same concentration after the same period of time (CLP = 93%) [44]. Furthermore, in our study, thirty days after GUH-2 instillations, a second mortality wave decreased considerably this survival rate (CLP-GUH-2 = 44%), which remained much lower than the one obtained with *P. aeruginosa.* When extrapolated to humans, these differences in behavior become of high importance in diseases in which both *N. cyriacigeorgica* and *P. aeruginosa* may cohabit. This has been the case in some patients with cystic fibrosis, as reported by Rodriguez-Nava et al. [2]. Traditionally, in these cases, primary antibiotic treatments will target *P. aeruginosa* because it is considered the main pathogen associated with lung deteriorations. Our study shows that the infective process of *N. cyriacigeorgica* must not be underestimated and that a treatment targeting both pathogens should be performed. This strategy has already been applied, and improved the clinical outcomes [2].

It is to be noted that based on this study, a small window of immunoparalysis due to CLP in mice was found sufficient to promote the colonization, persistence and dissemination of *N. cyriacigeorgica*. This observation could also be extrapolated to humans for which during a period of illness, the immune system of the patients is weak (diabetes, cancer, etc.) allowing the colonization of *Nocardia* in the infected organ during this "immunosuppressive window". Indeed, some patients considered immunocompetent may have had a history of disease [61]. So, according to our observations, we can state that locations presenting environmental conditions similar to the studied UIB in terms of humidity and metallic trace elements, may suppose an infective risk for weak populations.

Our study presents some limitations. For example, we studied a single UIB with its own geological, hydrological, chemical and vegetative characteristics. We must then be prudent in extrapolating the obtained results to any other UIBs. In this work, we compared the virulence of clinical and environmental strains of *N. cyriacigeorgica*, however just a single representative of each has been chosen. So, obtained conclusions should be carefully extrapolated to all *N. cyriacigeorgica* clinical and environmental strains.

However, our work has several strengths. For the first time, an urban, humid and polluted environment (an UIB) was used to study the spatiotemporal distribution of pathogens such as *N. cyriacigeorgica*. Moreover, we used the MLSA approach with precise gene concatenation (*rrs-hsp65-sodA-secA1*) to identify clonal lineages between clinical and environmental strains of *N. cyriacigeorgica*. In addition, according to the results obtained in this approach, it may be possible that *N. cyriacigeorgica* were a complex and not a single species, taking into account the presence of three MLSA-phylogroups whose taxonomy levels remains to be specified. We used, for the first time, the *hsp65* marker for the metabarcoding approach, allowing us to evaluate *Nocardia* biodiversity and to directly detect *N. cyriacigeorgica* in the urban sediments of an UIB. This new marker could also be used to track *Nocardia* in other environments. For the first time, the hazardousness of an environmental strain of *N. cyriacigeorgica* isolated from an UIB was studied by complete genome sequencing and by a murine model of transient immunoparalysis, which better mimics the population most frequently targeted by this pathogen.

5. Conclusion

This study presents, for the first time, a complete inventory of *Nocardia* causative agents of human nocardiosis found in a HAP-polluted urban infiltration system. This study was made possible by the development of an innovative metabarcoding *hsp65*-based approach. This led to the detection of the highly frequent species found in nocardiosis worldwide such as *N. cyriacigeorgica*, *N. nova*, and *N. abscessus*. The number of reads per species were found related with the field conditions. *N. cyriacigeorgica* was the most abundant pathogenic species, which makes this species the most worrisome in this kind of environments taking into account its epidemiologic characteristics. This led us to perform rounds of isolation of this bacterial species, and investigate more deeply their molecular epidemiology. A MLSA approach demonstrated a close proximity between the SIS *N. cyriacigeorgica* isolates and the clinical ones. However, these strains were mostly distributed in MLSA-phylogroup III, and not recorded in the MLSA-phylogroup II harboring the most virulent isolate recorded so far *i.e.* GUH-2. This suggested a significant diversification between these strains that could be indicative of a distinct tropism for the human host. This led us to compare the full genome of one SIS isolate with the one of GUH-2. No distinction in their virulence gene contents could be made, suggesting similar virulence potentialities. Experimentations were performed to test the virulence differences among these strains (and MLSA-phylogroups). GUH-2 strain was shown to be the most virulent isolate in an immunoparalysis CLP mice model but EML446, the SIS isolate, was also confirmed to be significantly virulent. This fact further supports the idea that all strains of this species can be pathogenic but with variable clinical outcomes. The GUH-2 lineage seems to be on-going an adaptation for animal hosts including humans. These differentiations linking MLSA-phylogroups and virulence will now need to be tested on a larger number of strains. The presence of pathogenic *Nocardia* is positively correlated to metallic trace elements and they can be suggested to be indicators of their presence. On the other hand, we have observed a negative correlation between PAHs and relative abundance pathogenic *Nocardia*, so these pollutants cannot be used as indicators of these bacteria. Overall, this study shows that humid and polluted environments such as UIBs may represent a health hazard for adjacent populations through either direct exposure or through an aerosolization of dusts harboring *N. cyriacigeorgica* cells.

CRediT authorship contribution statement

Florian Vautrin: Methodology, Writing, Investigation. **Petar Pujic:** Investigation. **Christian Paquet:** Investigation. **Emmanuelle Bergeron:** Investigation. **Delphine Mouniée:** Investigation. **Thierry Marchal:** Investigation. **Hélène Salord:** Investigation. **Jeanne-Marie Bonnet:** Validation. **Benoit Cournoyer:** Validation. **Thierry Winiarski:** Methodology. **Vanessa Louzier:** Supervision. **Veronica Rodriguez-Nava:** Supervision, Writing - review & editing.

Declaration of Competing Interest

The authors declare that they have no known competing financial interests or personal relationships that could have appeared to influence the work reported in this paper.

Acknowledgements

Florian Vautrin held a doctoral fellowship from the Auvergne-Rhône-Alpes region. The authors thank the Institut Claude Bourgelat – Biovivo of VetAgro Sup for animal facilities and the OTHU (Field Observatory for Urban Water Management, http://www.graie.org) for access to the infiltration basin. The authors are grateful to Béatrice Charton for her technical support on the *Nocardia* PCR detection, Audrey Dubost and Danis Abrouk for their bioinformatics knowledge, Christophe Martin for the first isolation of *N. cyriacigeorgica* environmental strain, Eva Gutbraut for her help with the electronic microscopy image and Jordan Brun for his technical support in bacteriology experiment. Abe Heme for his review and editorial assistance and Gonzalo Bermejo Miranda for his English grammar revision and Abe Hèm. The authors are also grateful to the Agence Nationale de la Recherche and LabEx IMU (Intelligence des Mondes Urbains) for their help in funding this work.

Source of funding

This work was partly funded by l'Agence Nationale de la Recherche through ANR-17-CE04-0010 (Infiltron) project, the Greater-Lyon Urban Community, the French national research program for environmental and occupational health of Anses under the terms of project "Iouqmer" EST 2016/1/120, the School of Integrated Watershed Sciences H2O'LYON (ANR 17-EURE-0018), and the Urban School of Lyon. Funders did not interfere in the elaboration of the experiments or data analysis.

Appendix A. Supplementary data

Supplementary data to this article can be found online at https://doi.org/10.1016/j.csbj.2020.12.017.

References

[1] Brown-Elliott BA, Brown JM, Conville PS, Wallace Jr RJ. Clinical and Laboratory Features of the *Nocardia* spp. Based on Current Molecular Taxonomy. CMR 2006;19(2):259–82. https://doi.org/10.1128/CMR.19.2.259-282.2006.

[2] Rodriguez-Nava V, Durupt S, Chyderiotis S, Freydière A-M, Karsenty J, de Montclos M, Reix P, Durieu I, Nove-Josserand R, Chiron R, Bremont F, Têtu L, Murris M, Terru D, Godreuil S, Bergeron E, Freney J, Boiron P, Vandenesch F, Marchandin H, Segonds C, Doléans-Jordheim A. A French multicentric study and review of pulmonary *Nocardia* spp. in cystic fibrosis patients. Med Microbiol Immunol 2015;204(4):493–504. https://doi.org/10.1007/s00430-014-0360-3.

[3] Heise ER. Diseases associated with immunosuppression.. Environ Health Perspect 1982;43:9–19. https://doi.org/10.1289/ehp.82439.

[4] Luo Q, Hiessl S, Poehlein A, Daniel R, Steinbüchel A, Loeffler FE. Insights into the microbial degradation of rubber and gutta-percha by analysis of the complete genome of *Nocardia nova* SH22a. Appl Environ Microbiol 2014;80(13):3895–907. https://doi.org/10.1128/AEM.00473-14.

[5] Luo Q, Hiessl S, Steinbüchel A. Functional diversity of Nocardia in metabolism: metabolism of nocardia. Environ Microbiol 2014;16(1):29–48. https://doi.org/10.1111/1462-2920.12221.

[6] Quatrini P, Scaglione G, Pasquale CD, Riela S, Puglia AM. 2008. Isolation of Gram-positive n-alkane degraders from a hydrocarbon-contaminated Mediterranean shoreline. J Appl Microbiol 104:251–259. https://doi.org/10.1111/j.1365-2672.2007.03544.x.

[7] Nhi-Cong LT, Mikolasch A, Awe S, Sheikhany H, Klenk H-P, Schauer F. Oxidation of aliphatic, branched chain, and aromatic hydrocarbons by Nocardia cyriacigeorgica isolated from oil-polluted sand samples collected in the Saudi Arabian Desert : oxidation of aliphatic, branched chain, and aromatic hydrocarbons by Nocardia cyriacigeorgica isolated from oil-polluted sand samples collected in the. J Basic Microbiol 2010;50(3):241–53. https://doi.org/10.1002/jobm.200900358.

[8] Pujic P, Beaman BL, Ravalison M, Boiron P, Rodríguez-Nava V. 2015. Chapter 40 - Nocardia and Actinomyces, p. 731–752. In Tang, Y-W, Sussman, M, Liu, D, Poxton, I, Schwartzman, J (eds.), Molecular Medical Microbiology (Second Edition). Academic Press, Boston. https://doi.org/10.1016/B978-0-12-397169-2.00040-8.

[9] Schlaberg R, Huard RC, Della-Latta P. *Nocardia cyriacigeorgica*, an Emerging Pathogen in the United States. J Clin Microbiol 2008;46(1):265–73. https://doi.org/10.1128/JCM.00937-07.

[10] Valdezate S, Garrido N, Carrasco G, Medina-Pascual MJ, Villalón P, Navarro AM, Saéz-Nieto JA. 2016. Epidemiology and susceptibility to antimicrobial agents of the main Nocardia species in Spain. J Antimicrob Chemother dkw489. https://doi.org/10.1093/jac/dkw489

[11] Lebeaux D, Bergeron E, Berthet J, Djadi-Prat J, Mouniée D, Boiron P, Lortholary O, Rodriguez-Nava V. Antibiotic susceptibility testing and species identification of *Nocardia* isolates: a retrospective analysis of data from a French expert laboratory, 2010–2015. Clin Microbiol Infect 2019;25(4):489–95. https://doi.org/10.1016/j.cmi.2018.06.013.

[12] Bernardin-Souibgui C, Barraud S, Bourgeois E, Aubin J-B, Becouze-Lareure C, Wiest L, Marjolet L, Colinon C, Lipeme Kouyi G, Cournoyer B, Blaha D. Incidence of hydrological, chemical, and physical constraints on bacterial pathogens, *Nocardia* cells, and fecal indicator bacteria trapped in an urban stormwater detention basin in Chassieu, France. Environ Sci Pollut Res 2018;25(25):24860–81. https://doi.org/10.1007/s11356-018-1994-2.

[13] M. Rahmati L. Weihermüller J. Vanderborght Y.A. Pachepsky L. Mao S.H. Sadeghi N. Moosavi H. Kheirfam C. Montzka K. Van Looy B. Toth Z. Hazbavi W. Al Yamani A.A. Albalasmeh M.Z. Alghzawi R. Angulo-Jaramillo A.C.D. Antonino G. Arampatzis R.A. Armindo H. Asadi Y. Bamutaze J. Batlle-Aguilar B. Béchet F. Becker G. Blöschl K. Bohne I. Braud C. Castellano A. Cerdà M. Chalhoub R. Cichota M. Císlerová B. Clothier Y. Coquet W. Cornelis C. Corradini A.P. Coutinho M.B. de Oliveira J.R. de Macedo M.F. Durães H. Emami I. Eskandari A. Farajnia A. Flammini N. Fodor M. Gharaibeh M.Rahmati M, Weihermüller L, Vanderborght J, Pachepsky YA, Mao L, Sadeghi SH, Moosavi N, Kheirfam H, Montzka C, Van Looy K, Toth B, Hazbavi Z, Al Yamani W, Albalasmeh AA, Alghzawi MZ, Angulo-Jaramillo R, Antonino ACD, Arampatzis G, Armindo RA, Asadi H, Bamutaze Y, Batlle-Aguilar J, Béchet B, Becker F, Blöschl G, Bohne K, Braud I, Castellano C, Cerdà A, Chalhoub M, Cichota R, Císlerová M, Clothier B, Coquet Y, Cornelis W, Corradini C, Coutinho AP, de Oliveira MB, de Macedo JR, Durães MF, Emami H, Eskandari I, Farajnia A, Flammini A, Fodor N, Gharaibeh M, Ghavimipanah MH, Ghezzehei TA, Giertz S, Hatzigiannakis EG, Horn R, Jiménez JJ, Jacques D, Keesstra SD, Kelishadi H, Kiani-Harchegani M, Kouselou M, Kumar Jha M, Lassabatere L, Li X, Liebig MA, Lichner L, López MV, Machiwal D, Mallants D, Mallmann MS, de Oliveira Marques JD, Marshall MR, Mertens J, Meunier F, Mohammadi MH, Mohanty BP, Pulido-Moncada M, Montenegro S, Morbidelli R, Moret-Fernández D, Moosavi AA, Mosaddeghi MR, Mousavi SB, Mozaffari H, Nabiollahi K, Neyshabouri MR, Ottoni MV, Ottoni Filho TB, Pahlavan-Rad MR, Panagopoulos A, Peth S, Peyneau P-E, Picciafuoco T, Poesen J, Pulido M, Reinert DJ, Reinsch S, Rezaei M, Roberts FP, Robinson D, Rodrigo-Comino J, Rotunno Filho OC, Saito T, Suganuma H, Saltalippi C, Sándor R, Schütt B, Seeger M, Sepehrnia N, Sharifi Moghaddam E, Shukla M, Shutaro S, Sorando R, Stanley AA, Strauss P, Su Z, Taghizadeh-Mehrjardi R, Taguas E, Teixeira WG, Vaezi AR, Vafakhah M, Vogel T, Vogeler I, Votrubova J, Werner S, Winarski T, Yilmaz D, Young MH, Zacharias S, Zeng Y, Zhao Y, Zhao H, Vereecken H. 2018. Development and analysis of the Soil Water Infiltration Global database. Earth Syst Sci Data 10:1237–1263. https://doi.org/10.5194/essd-10-1237-2018.

[14] Sébastian C, Barraud S, Ribun S, Zoropogui A, Blaha D, Becouze-Lareure C, Kouyi GL, Cournoyer B. Accumulated sediments in a detention basin: chemical and microbial hazard assessment linked to hydrological processes. Environ Sci Pollut Res 2014;21(8):5367–78. https://doi.org/10.1007/s11356-013-2397-z.

[15] Badin AL, Monier A, Volatier L, Geremia RA, Delolme C, Bedell J-P. Structural stability, microbial biomass and community composition of sediments affected by the hydric dynamics of an urban stormwater infiltration basin: dynamics of physical and microbial characteristics of stormwater sediment. Microb Ecol 2011;61(4):885–97. https://doi.org/10.1007/s00248-011-9829-4.

[16] Marti R, Bécouze-Lareure C, Ribun S, Marjolet L, Bernardin Souibgui C, Aubin J-B, Lipeme Kouyi G, Wiest L, Blaha D, Cournoyer B. Bacteriome genetic structures of urban deposits are indicative of their origin and impacted by chemical pollutants. Sci Rep 2017;7(1). https://doi.org/10.1038/s41598-017-13594-8.

[17] Kaushik R, Balasubramanian R, de la Cruz AA. Influence of air quality on the composition of microbial pathogens in fresh rainwater. Appl Environ Microbiol 2012;78(8):2813–8. https://doi.org/10.1128/AEM.07695-11.

[18] Barraud S, Gibert J, Winiarski T, Krajewski J-LB. 2002. Implementation of a monitoring system to measure impact of stormwater runoff infiltration. Water Sci Technol 45:203–210. https://doi.org/10.2166/wst.2002.0080.

[19] Winiarski T. 2014. Fonction filtration d'un ouvrage urbain - consequence sur la formation d'un anthroposol. 2015. Available: http://temis.documentation.developpement-durable.gouv.fr/docs/Temis/0081/Temis-0081850/21970_A.pdf 199 p [accessed 19 April 2019].

[20] Li J, Shang Xu, Zhao Z, Tanguay RL, Dong Q, Huang C. Polycyclic aromatic hydrocarbons in water, sediment, soil, and plants of the Aojiang River waterway in Wenzhou, China. J Hazard Mater 2010;173(1-3):75–81. https://doi.org/10.1016/j.jhazmat.2009.08.050.

[21] Muntean N, Muntean E, Duda MM. 2015. Polycyclic Aromatic Hydrocarbons in Soil. ResearchGate.

[22] Rodriguez-Nava V, Couble A, Devulder G, Flandrois J-P, Boiron P, Laurent F. Use of PCR-restriction enzyme pattern analysis and sequencing database for *hsp65*

gene-based identification of *Nocardia* species. J Clin Microbiol 2006;44 (2):536–46. https://doi.org/10.1128/JCM.44.2.536-546.2006.
[23] Telenti A, Marchesi F, Balz M, Bally F, Böttger EC, Bodmer T. 1993. Rapid identification of mycobacteria to the species level by polymerase chain reaction and restriction enzyme analysis. J Clin Microbiol 31:175–178.
[24] Sánchez-Herrera K, Sandoval H, Mouniee D, Ramírez-Durán N, Bergeron E, Boiron P, Sánchez-Saucedo N, Rodríguez-Nava V. Molecular identification of *Nocardia* species using the *sod* A gene. New Microbes New Infect 2017;19:96–116. https://doi.org/10.1016/j.nmni.2017.03.008.
[25] Conville PS, Zelazny AM, Witebsky FG. Analysis of *secA1* gene sequences for identification of *Nocardia* Species. J Clin Microbiol 2006;44(8):2760–6. https://doi.org/10.1128/JCM.00155-06.
[26] Laurent FJ, Provost F, Boiron P. 1999. Rapid Identification of Clinically Relevant Nocardia Species to Genus Level by 16S rRNA Gene PCR. J Clin Microbiol 37:99–102.
[27] Verzani J. Using R for introductory statistics. Chapman and Hall/CRC 2004. https://doi.org/10.4324/9780203499894.
[28] Charif D, Thioulouse J, Lobry JR, Perri G, re. Online synonymous codon usage analyses with the ade4 and seqinR packages. Bioinformatics 2005;21 (4):545–7. https://doi.org/10.1093/bioinformatics/bti037.
[29] Lê Cao K-A, Boitard S, Besse P. Sparse PLS discriminant analysis: biologically relevant feature selection and graphical displays for multiclass problems. BMC Bioinf 2011;12(1). https://doi.org/10.1186/1471-2105-12-253.
[30] Friendly M. Corrgrams: exploratory displays for correlation matrices. Am Statist 2002;56(4):316–24. https://doi.org/10.1198/000313002533.
[31] Schloss PD, Westcott SL, Ryabin T, Hall JR, Hartmann M, Hollister EB, Lesniewski RA, Oakley BB, Parks DH, Robinson CJ, Sahl JW, Stres B, Thallinger GG, Van Horn DJ, Weber CF. Introducing mothur: open-Source, platform-independent, community-supported software for describing and comparing microbial communities. AEM 2009;75(23):7537–41. https://doi.org/10.1128/AEM.01541-09.
[32] Beaman BL, Maslan S. 1977. Effect of cyclophosphamide on experimental Nocardia asteroides infection in mice. Infect Immun 16:995–1004.
[33] Yassin AF, Rainey FA, Steiner U. 2001. Nocardia cyriacigeorgici sp. nov.. Int J Syst Evol Microbiol 51:1419–1423. https://doi.org/10.1099/00207713-51-4-1419
[34] Gouy M, Guindon S, Gascuel O. Seaview version 4: a multiplatform graphical user interface for sequence alignment and phylogenetic tree building. Mol Biol Evol 2010;27(2):221–4. https://doi.org/10.1093/molbev/msp259.
[35] McTaggart LR, Richardson SE, Witkowska M, Zhang SX. Phylogeny and identification of *Nocardia* species on the basis of multilocus sequence analysis. J Clin Microbiol 2010;48(12):4525–33. https://doi.org/10.1128/JCM.00883-10.
[36] Rudramurthy SM, Kaur H, Samanta P, Ghosh A, Chakrabarti A, Honnavar P, Ray P. 2015. Molecular identification of clinical Nocardia isolates from India. J Med Microbiol 64:1216–1225. https://doi.org/10.1099/jmm.0.000143
[37] Xiao M, Pang L, Chen SC-A, Fan X, Zhang L, Li H-X, Hou X, Cheng J-W, Kong F, Zhao Y-P, Xu Y-C. 2016. Accurate Identification of Common Pathogenic Nocardia Species: Evaluation of a Multilocus Sequence Analysis Platform and Matrix-Assisted Laser Desorption Ionization-Time of Flight Mass Spectrometry. PLOS ONE 11:e0147487. https://doi.org/10.1371/journal.pone.0147487.
[38] Kumar S, Stecher G, Tamura K. MEGA7: molecular evolutionary genetics analysis version 7.0 for bigger datasets. Mol Biol Evol 2016;33(7):1870–4. https://doi.org/10.1093/molbev/msw054.
[39] Gilbert B, McDonald IR, Finch R, Stafford GP, Nielsen AK, Murrell JC. Molecular analysis of the pmo (particulate methane monooxygenase) operons from two type II methanotrophs. Appl Environ Microbiol 2000;66(3):966–75. https://doi.org/10.1128/AEM.66.3.966-975.2000.
[40] Vallenet D, Calteau A, Cruveiller S, Gachet M, Lajus A, Josso A, Mercier J, Renaux A, Rollin J, Rouy Z, Roche D, Scarpelli C, Médigue C. MicroScope in 2017: an expanding and evolving integrated resource for community expertise of microbial genomes. Nucleic Acids Res 2017;45(D1):D517–28. https://doi.org/10.1093/nar/gkw1101.
[41] Vautrin F, Bergeron E, Dubost A, Abrouk D, Martin C, Cournoyer B, Louzier V, Winiarski T, Rodriguez-Nava V, Pujic P, Newton ILG. Genome sequences of three *Nocardia cyriacigeorgica* strains and one *Nocardia asteroides* strain. Microbiol Resour Announc 2019;8(33). https://doi.org/10.1128/MRA.00600-19.
[42] Zoropogui A, Pujic P, Normand P, Barbe V, Belli P, Graindorge A, Roche D, Vallenet D, Mangenot S, Boiron P, Rodriguez-Nava V, Ribun S, Richard Y, Cournoyer B, Blaha D. The *Nocardia cyriacigeorgica* GUH-2 genome shows ongoing adaptation of an environmental Actinobacteria to a pathogen's lifestyle. BMC Genomics 2013;14(1):286. https://doi.org/10.1186/1471-2164-14-286.
[43] Restagno D, Venet F, Paquet C, Freyburger L, Allaouchiche B, Monneret G, Bonnet J-M, Louzier V. 2016. Mice Survival and Plasmatic Cytokine Secretion in a "Two Hit" Model of Sepsis Depend on Intratracheal Pseudomonas Aeruginosa Bacterial Load. PLoS ONE 11. https://doi.org/10.1371/journal.pone.0162109
[44] Nemzek JA, Xiao H-Y, Minard AE, Bolgos GL, Remick DG. 2004. Humane endpoints in shock research. Shock Augusta Ga 21:17–25. https://doi.org/10.1097/01.shk.0000101667.49265.fd
[45] Feldman AT, Wolfe D. Tissue processing and hematoxylin and eosin staining. In: Histopathology. New York, NY: Humana Press; 2014. p. 31–43. https://doi.org/10.1007/978-1-4939-1050-2_3.
[46] Wang Q, Garrity GM, Tiedje JM, Cole JR. Naïve bayesian classifier for rapid assignment of rRNA sequences into the new bacterial taxonomy. Appl Environ Microbiol 2007;73:5261–7. https://doi.org/10.1128/AEM.00062-07.
[47] Cui Q, Fang T, Huang Y, Dong P, Wang H. Evaluation of bacterial pathogen diversity, abundance and health risks in urban recreational water by amplicon next-generation sequencing and quantitative PCR. J Environ Sci 2017;57:137–49. https://doi.org/10.1016/j.jes.2016.11.008.
[48] Fan C, Li Y, Liu P, Mu F, Xie Z, Lu R, Qi Y, Wang B, Jin C. Characteristics of airborne opportunistic pathogenic bacteria during autumn and winter in Xi'an, China. Sci Total Environ 2019;672:834–45. https://doi.org/10.1016/j.scitotenv.2019.03.412.
[49] Arrache D, Zait H, Rodriguez-Nava V, Bergeron E, Durand T, Yahiaoui M, Grenouillet F, Amrane A, Chaouche F, Baiod A, Madani K, Hamrioui B. Nocardiose cérébrale et pulmonaire à *Nocardia abscessus* chez un patient algérien immunocompétent. J Mycol Méd 2018;28(3):531–7. https://doi.org/10.1016/j.mycmed.2018.04.010.
[50] Garcia-Bellmunt L, Sibila O, Solanes I, Sanchez-Reus F, Plaza V. Pulmonary nocardiosis in patients With COPD: characteristics and prognostic factors. Arch Bronconeumol (English Edition) 2012;48(8):280–5. https://doi.org/10.1016/j.arbr.2012.06.006.
[51] Steinbrink J, Leavens J, Kauffman CA, Miceli MH. 2018. Manifestations and outcomes of nocardia infections: Comparison of immunocompromised and nonimmunocompromised adult patients. Medicine (Baltimore) 97:e12436. https://doi.org/10.1097/MD.0000000000012436.
[52] Eshraghi SS, Heidarzadeh S, Soodbakhsh A, Pourmand M, Ghasemi A, GramiShoar M, Zibafar E, Aliramezani A. Pulmonary nocardiosis associated with cerebral abscess successfully treated by co-trimoxazole: a case report. Folia Microbiol 2014;59(4):277–81. https://doi.org/10.1007/s12223-013-0298-7.
[53] Budzinski H, Garrigues Ph, Connan J, Devillers J, Domine D, Radke M, Oudins JL. Alkylated phenanthrene distributions as maturity and origin indicators in crude oils and rock extracts. Geochim Cosmochim Acta 1995;59(10):2043–56. https://doi.org/10.1016/0016-7037(95)00125-5.
[54] Yunker MB, Macdonald RW, Vingarzan R, Mitchell RH, Goyette D, Sylvestre S. PAHs in the fraser river basin: a critical appraisal of PAH ratios as indicators of PAH source and composition. Org Geochem 2002;33(4):489–515. https://doi.org/10.1016/S0146-6380(02)00002-5.
[55] Nádudvari Á, Fabiańska MJ. Coal-related sources of organic contamination in sediments and water from the Bierawka River (Poland). Int J Coal Geol 2015;152:94–109. https://doi.org/10.1016/j.coal.2015.11.006.
[56] Radke M, Welte DH, Willsch H. Maturity parameters based on aromatic hydrocarbons: Influence of the organic matter type. Org Geochem 1986;10(1-3):51–63. https://doi.org/10.1016/0146-6380(86)90008-2.
[57] Moran NA. Microbial minimalism. Cell 2002;108(5):583–6. https://doi.org/10.1016/S0092-8674(02)00665-7.
[58] McMahon MD, Rush JS, Thomas MG. Analyses of MbtB, MbtE, and MbtF suggest revisions to the mycobactin biosynthesis pathway in *Mycobacterium tuberculosis*. J Bacteriol 2012;194(11):2809–18. https://doi.org/10.1128/JB.00088-12.
[59] Li F, Feng L, Jin C, Wu X, Fan L, Xiong S, Dong Y. LpqT improves mycobacteria survival in macrophages by inhibiting TLR2 mediated inflammatory cytokine expression and cell apoptosis. Tuberculosis 2018;111:57–66. https://doi.org/10.1016/j.tube.2018.05.007.
[60] Cruz-Rabadán JS, Miranda-Ríos J, Espín-Ocampo G, Méndez-Tovar LJ, Maya-Pineda HR, Hernández-Hernández F. Non-coding RNAs are differentially expressed by nocardia brasiliensis in vitro and in experimental actinomycetoma. TOMICROJ 2017;11(1):112–25. https://doi.org/10.2174/1874285801711010112.
[61] Singh I, West FM, Sanders A, Hartman B, Zappetti D. Pulmonary nocardiosis in the immunocompetent host: case series. Case Rep Pulmonol 2015;2015:1–6. https://doi.org/10.1155/2015/314831.